

RECONFIGURABLE ELECTROCHEMICAL BIOSENSOR ENABLED BY DIGITAL
MICROFLUIDIC DEVICES

by

ALI FARZBOD

Presented to the Faculty of the Graduate School of
The University of Texas at Arlington in Partial Fulfillment
of the Requirements
for the Degree of

DOCTOR OF PHILOSOPHY

THE UNIVERSITY OF TEXAS AT ARLINGTON

April 2018

Copyright © by Ali Farzbod 2018

All Rights Reserved



Acknowledgments

I would like to dedicate this dissertation to my father who has always been supportive in all my academic endeavors, to my wife and my siblings for their blessings and my friends, colleagues for their support and encouragement throughout my research.

I would like to thank my advisor, Prof. Hyejin Moon for giving me the opportunity to join her lab and always encourage me to think out of the box. Her openness to innovation and experimentation with new and existing resources made research fun and exciting. I always found her intellectual, personable and helpful – traits which make her my role model in my life.

The University of Texas at Arlington (UTA) had been my second home for many years and had excellent resources at my disposal.

I thank the President, Dean of the College of Engineering (CoE), professors, administrative staff and the management across various departments who were responsible for my success in pursuing a Ph.D. degree at this outstanding university.

Lastly, A big thank you to my committee members, Dr. Ashfagh Adnan, Dr. Cheng Luo, Dr. Digant Dave and Dr. Kyungsuk Yum for their help and support throughout the projects.

April 12, 2018

Abstract

RECONFIGURABLE ELECTROCHEMICAL BIOSENSOR ENABLED BY DIGITAL MICROFLUIDIC DEVICES

Ali Farzbod, PhD

The University of Texas at Arlington, 2018

Supervising Professor: Hyejin Moon

The increasing demand for improving the health care quality in developed countries with synchronous advances in the microfabrication of CMOS devices results in the emergence of the Lab-on-a-chip (LOC) field. The ultimate goal of LOC's is to achieve the complete integration of biomedical protocols, such as sample pre-processing and separation and analysis of biosamples on a chip.

Electrowetting on dielectric (EWOD) as a distinctive digital microfluidic (DMF) is capable of manipulating droplets less than a microliter along the electrode arrays by applying AC voltages. EWOD chips, as microfluidic platforms, are inherently electrical and do not have to deal with problems regarding a hydraulic system. Additionally, this feature makes them more compatible with control and feedback circuits while entailing their fabrication to be similar to well-developed CMOS fabrication. Another feature of these devices is the capability to control the very small volume of liquid (up to 900 nl), which becomes extremely important when working with expensive reagents, especially in bioanalysis. In the first part of this study, we present a demonstration of a reconfigurable potentiometric ion-selective electrode (ISE) array enabled by an electrowetting-on-dielectric (EWOD) microfluidic platform. This reconfigurability required the proposed sensor to be made on the EWOD chip and removed after use. The on-chip fabrication of

the potassium ion-selective sensor includes electroplating Ag followed by forming an AgCl layer by chemical oxidation and forming a thin layer of polymer-based potassium ion-selective membrane on one of the sensor electrodes. The proposed device with the capability of on-chip ISE fabrication has many advantages such as automation, longer lifetime, minimal membrane and sample consumption, which makes it an outstanding candidate for a portable home-use device for regular measurements of human blood panels. In the second part of the study, the focus was on simultaneous measurement of potassium, sodium and calcium ions in a drop of emulated blood plasma sample via an EWOD microfluidic chip to deliver a showcase for the potential use of these devices for regular screening of blood panels such as electrolyte panels. In the last part of the study, we focused more on tackling a major problem of most biosensors known as immobilization. The goal was to eliminate the immobilization process on sensor electrodes by introducing a reconfigurable liquid-liquid electrochemical sensor which is compatible with EWOD platforms. In this sensor, at first, one droplet (ionic liquid) containing potassium selective ionophore was dispensed over an interdigitated electrode. By acquiring a first electro impedance spectra (EIS) and fitting it to our equivalent circuit model, the initial values of electrical parameters of our modified ionic liquid were calculated. Then a drop of the sample solution containing the targeted biological molecule was dispensed over next to the modified liquid to create a liquid-liquid junction. Due to the specific affinity of the bio-receptor (i.e., biological recognition molecules), the targeted biomolecule will attach or transfer to the selective medium (i.e., modified droplet). Finally, by removing the sample liquid from the interface, we perform another EIS to find the secondary value of components of the equivalent circuit of modified liquid. The difference between the initial and secondary values of electrical elements correlated to the concentration of the targeted biomolecule in the sample solution.

Table of Contents

| | |
|--|-----|
| Acknowledgments | iii |
| Abstract | iv |
| List of Illustrations | ix |
| List of Tables | xii |
| Chapter 1 Introduction..... | 13 |
| 1.1 Electrowetting on Dielectric (EWOD)..... | 13 |
| 1.2 Electrochemical Bio-sensors | 15 |
| 1.2.1 Measurement Techniques | 17 |
| 1.2.2 Immobilization of a biological recognition element..... | 17 |
| 1.3 Ion-selective sensor..... | 19 |
| 1.3.1 Reference electrode | 21 |
| 1.3.2 Ion-Selective Membrane (ISM)..... | 21 |
| 1.3.3 Nernst Equation..... | 23 |
| 1.4 Electro impedance spectroscopy..... | 24 |
| 1.5 Ionic Liquids..... | 27 |
| Chapter 2 Integration of a reconfigurable electrochemical sensor into a digital microfluidic platform | 29 |
| 2.1 Literature summary & motivation..... | 29 |
| 2.2 Materials & Methods | 31 |
| 2.2.1 Materials | 31 |
| 2.2.2 Sensor design and configuration of the EWOD-electrochemical cell | 32 |
| 2.2.3 EWOD Chip Fabrication | 34 |
| 2.2.3.1 EWOD Chip Fabrication reactive ion etching | 37 |

| | |
|--|-------------------------------------|
| 2.2.3.2 EWOD Chip Fabrication-SU-8 mask & electroplating | 38 |
| 2.2.3.3 On-chip fabrication & calibration of potassium ion selective sensor | 41 |
| 2.3 Results and Discussion | 42 |
| 2.3.1 On-chip Fabrication of Ag/AgCl reference electrodes | 42 |
| 2.3.2 On-chip formation of Potassium ion selective membrane..... | 43 |
| 2.3.3 Calibration | 44 |
| 2.4 Conclusion & Outlook | 47 |
| Chapter 3 Simultaneous measurement of K ⁺ , Na ⁺ and Ca ²⁺ concentrations in a droplet of a human blood plasma emulated solution | 49 |
| 3.1 Motivation | 49 |
| 3.2 Material & Methods..... | 51 |
| 3.2.1 Material..... | 51 |
| 3.2.2 Off-chip Formation & calibration potentiometric sensor assay..... | 52 |
| 3.3 Results & Discussion | 53 |
| 3.3.1 Off-chip calibration of sodium selective sensor | 53 |
| 3.3.2 Off-chip calibration of calcium selective sensor | 56 |
| 3.3.3 Simultaneous measurement multiple ions via EWOD chip | 58 |
| 3.3 Conclusion & outlook | 61 |
| Chapter 4 Towards liquid-liquid electrochemical bio-sensor enabled by an EWOD Platform..... | 62 |
| 4.1 Literature summary & motivation..... | 62 |
| 4.2 Material & Methods..... | 63 |
| 4.2.1 Material..... | 65 |
| 4.2.2 Sensing Scheme | Error! Bookmark not defined. |

| | |
|---|----|
| 4.2.2 Sensor Design & equivalent circuit model considerations | 67 |
| 4.3 Initial results and discussion | 73 |
| 4.4 Conclusion & outlook | 76 |
| Chapter 5 Conclusion..... | 77 |
| References..... | 78 |
| Biographical Information | 84 |

List of Illustrations

| | |
|---|----|
| Figure 1-1 Principle of electrowetting. (a) No external voltage applied. Charges are distributed at the electrode-electrolyte interface, building an electric double layer (EDL). (b) An external voltage applied. Charge density at EDL changes so that γ_{SL} and the contact angle decrease or increase..... | 14 |
| Figure 1-2 Elements of a Biosensor[6]..... | 15 |
| Figure 1-3 Schematic of Immobilization techniques[8] | 19 |
| Figure 1-4 Schematic of a macroscale ISE..... | 20 |
| Figure 1-5 Nyquist Plot with impedance Vector[13]..... | 26 |
| Figure 1-6 Bode plot with one time constant[13] | 26 |
| Figure 2-1 Schematics of an electrochemical cell integrated with EWOD electrodes..... | 32 |
| Figure 2-2 Fabrication process of the bottom chip of an EWOD DMF device..... | 36 |
| Figure 2-3 Characterization of the etching rate of the RIE of Teflon. (a) Sample preparation method for RIE characterization. (b) Thickness Vs. Time..... | 37 |
| Figure 2-4 A scan of sensor electrode integrated with EWOD electrode | 38 |
| Figure 2-5 (a) Initial sensor design (sensor edges are open to the electric field), (b) enhanced design (Su8 covering the edges of sensor electrode) | 40 |
| Figure 2-6 Electroplating thickness characterization;(a) before electroplating, and (b) after electroplating..... | 40 |
| Figure 2-7 On-chip ion-selective electrodes fabrication and calibration procedure. Step (1) is dispensing a droplet from Ag plating solution reservoir and transporting it to sensor electrode for electroplating Ag on patterned Au as seed layer, Step (2) is chemical oxidation of Ag layer with HCl solution using EWOD electrode for precise manipulations, Step (3) is forming a thin layer of ion-selective membrane on a sensor electrode and Step (4) is serial dilution for on-chip calibrating of the sensor (this step is proposal only)..... | 42 |

| | |
|--|----|
| Figure 2-8 On-chip electroplating of Ag demonstration. (a) Ag deposition on the left sensor electrode, and (b) Ag deposition on the right sensor electrode. | 43 |
| Figure 2-9 Top and side view of ISM solution pinching-off process. (a) an ISM solution droplet brought over a sensor electrode by EWOD motion, (b) the ISM solution droplet is being driven away from the sensor electrode while a part of ISM solution is wetting the hydrophilic opening over the electrode, and (c) a thin layer of ISM on sensor electrode after the completion of pinch-off and evaporating the solvent(THF)..... | 44 |
| Figure 2-10 EMF responses vs. time and Log(a) a) Measuring EMF (electromotive force) on EWOD with respect to time, b) Nernstian response to the different molarity of KCl solutions (calibration curve) | 46 |
| Figure 3-1 Schematic side view of the potentiometric sensor | 52 |
| Figure 3-2 Off-chip sensing platform (a) Actual Setup (b) Mask for patterning Au on wafers | 53 |
| Figure 3-3 Electromotive force measurement by the sodium selective sensor with respect to time..... | 54 |
| Figure 3-4 Calibration curve for average EMF (electromotive force) @ t=30 seconds | 55 |
| Figure 3-5 Electromotive force measurement by calcium selective sensor with respect to time..... | 56 |
| Figure 3-6 Calibration curve of Calcium ion selective sensor for average EMF (electromotive force) @ t=30 seconds | 57 |
| Figure 3-7 simultaneous measurement of Ca^{2+} , K^+ , Na^+ | 59 |
| Figure 3-8 Electromotive force measurement by Ca^{2+} , K^+ , Na^+ selective sensor with respect to time..... | 60 |
| Figure 4-1 Chemical formula of 1-Ethyl-3-methylimidazolium bis(trifluoromethylsulfonyl)imide..... | 66 |

| | |
|---|----|
| Figure 4-2 Liquid-liquid Testing scheme. a) The modified ionic liquid (liquid containing ionophore) dispensed over the sensing electrode, and an EIS acquired for determination of initial values. b) The sample solution dispensed over the next electrode, then with activation the central electrode an interface will form between 'modified liquid' and "sample liquid. c) By removing the sample liquid from the interface, another EIS acquired to find the secondary values | 64 |
| Figure 4-3 Interdigitated electrode integrated on EWOD electrode. a) Schematic of sensor b) Actual photo of IDE c) Sensing platform | 68 |
| Figure 4-4 Equivalent circuit for Initial EIS Data | 69 |
| Figure 4-5 Curve fitting of initial experimental data with the model (The bode plot) | 70 |
| Figure 4-6 Curve fitting of initial Experimental Data with model (The Nyquist plot)..... | 71 |
| Figure 4-7 Equivalent circuit for secondary EIS Data | 72 |
| Figure 4-8 Curve fitting of secondary experimental data with model (The bode plot) | 72 |
| Figure 4-9 Pure Ionic Liquid as a selective medium in LLE | 74 |
| Figure 4-10 Electro impedance spectroscopy of initial values..... | 74 |
| Figure 4-11 Impedance difference Vs. KCl sample concentration | 75 |

List of Tables

| | |
|--|----|
| Table 1-1 Types of receptors and measurement techniques in Biosensors[7]..... | 16 |
| Table 1-2 Measurement techniques in electrochemical sensors[7]..... | 17 |
| Table 1-3 Comparison of immobilization techniques[8] | 18 |
| Table 1-4 Common anions and cations in ILs[20] | 28 |
| Table 2-1 Electromotive responses of different molarities of KCL solutions in three experiments @ t=210s..... | 46 |
| Table 3-1 Serum elements of basic metabolic panel..... | 50 |
| Table 3-2 Serum elements of Lipid panel | 50 |
| Table 3-3 EMF responses of different molarities of NaCl solutions in three experiments @ t=30s. | 54 |
| Table 3-4 Electromotive responses of different molarities of CaCl ₂ solutions in three experiments @ t=30s..... | 57 |
| Table 4-1 physicochemical properties of 1-Ethyl-3-methylimidazolium bis(trifluoromethylsulfonyl)imide..... | 65 |
| Table 4-2 Standard deviations of initial impedance values of modified ionic liquid | 74 |

Chapter 1

Introduction

1.1 Electrowetting on Dielectric (EWOD)

Surface tension is an inherently dominant force in the micro scale, therefore, electrocapillarity based microfluidic devices such as EWOD shown their applicability and superiority in handling the discrete amount of liquid.

The principle of EWOD is the change in contact angle of a polarizable liquid drop when it is placed on an electrode coated with a dielectric layer, and an electric potential is applied across the droplet.

When an external electric potential is applied between a liquid and solid or between two immiscible liquids the charges and dipoles redistribute, modifying the surface energy at the solid/liquid interface or liquid/liquid[1] (Figure 1-1). The first phenomenon leads to the reduction of interface tension, whereas the second one leads to the change in the line tension and as thereby in the contact angle[2], in other words, applying voltage modify the equilibrium state of tension forces at the three-phase contact line causes liquid to wet the surface. An EWOD chip utilizes these wetting forces along the meniscus to drive for a microdroplet along an array of electrodes or a network of electrodes[3][4].

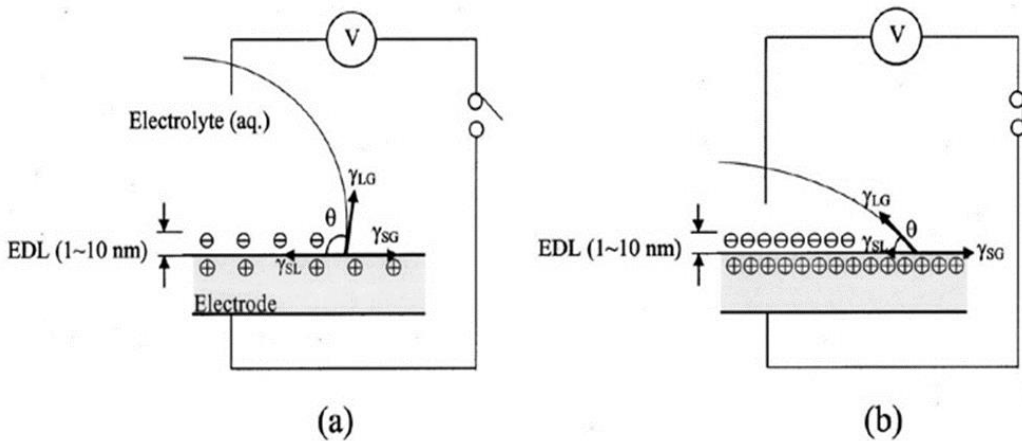


Figure 1-1 Principle of electrowetting. (a) No external voltage applied. Charges are distributed at the electrode-electrolyte interface, building an electric double layer (EDL). (b) An external voltage applied. Charge density at EDL changes so that γ_{SL} and the contact angle decrease or increase [1].

Young's equation relates the cosine of the equilibrium contact angle to the three interfacial tensions by:

$$\cos \theta = \frac{\gamma_{SV} - \gamma_{SL}}{\gamma_{LV}} \quad (1)$$

Where γ_{SV} , γ_{SL} , γ_{LV} are surface tensions of solid-vapor, solid-liquid, and liquid-vapor interfaces, respectively.

According to Lippmann equation, when the potential is applied at the interface, considering no change in $L-V$ and $S-V$ surface tensions, the change in solid-liquid surface tensions as follows[5]:

$$\gamma_{SL}(V) = \gamma_{SL}(0) - \frac{C_H}{2} V^2 \quad (2)$$

Where C_H is the Helmholtz capacitance per unit area of the solid-liquid interface (i.e., EDL capacitance).

Combining equation (1) and (2) gives the relationship between contact angle and the applied voltage, which is known as the Young-Lippmann equation shown equation (3).

$$\cos \theta = \cos \theta_0 + \frac{C_H}{2\gamma l v} V^2 \quad (3)$$

where θ and θ_0 are contact angles when the applied voltage is V and zero respectively.

1.2 Electrochemical Bio-sensors

Electrochemical biosensor provides selective quantitative or semi-quantitative analytical information utilizing a biological recognition molecule which is retained in direct spatial contact with an electrochemical transduction element (i.e., electrical interface).

Figure 1-2 explains the main components of an electrochemical biosensor.

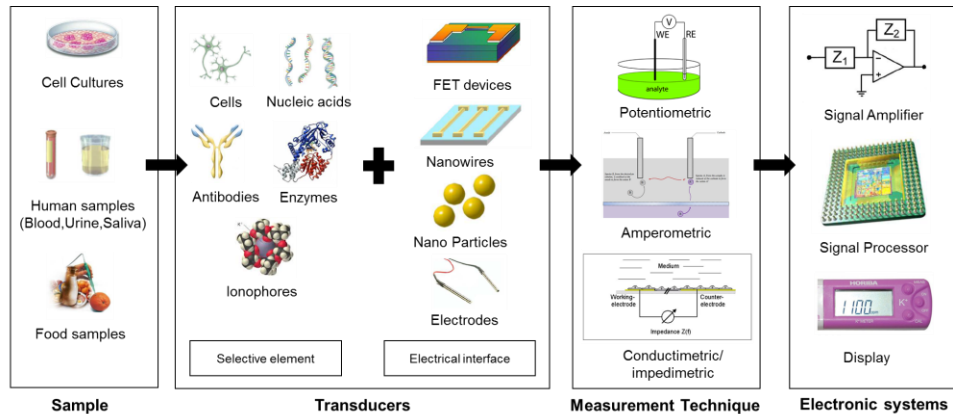


Figure 1-2 Elements of a Biosensor [6]

The selective element may be based on a chemical reaction catalyzed by, or on an equilibrium reaction with macromolecules that have been isolated, engineered or present in their original biological environment. Electrochemical biosensors may be further classified into two categories: Direct monitoring of analyte concentration or the targeted reactions in which the analyte consumed; alternatively, an inhibitor or activator can be used

for indirect monitoring of the biological recognition (selective) element. Table 1-1 shows the type of receptors and measurement techniques used for different kind of analyses.

Table 1-1 Types of receptors and measurement techniques in Biosensors[7]

| Analytes | Receptor/Chemical recognition system | Measurement technique/ Transduction mode |
|---|---|---|
| 1. Ions | Mixed valence metal oxides permselective, ion-conductive inorganic crystals | Potentiometric, voltammetric |
| | Trapped mobile synthetic or biological ionophores | |
| | Ion exchange glasses | |
| | Enzyme(s) | |
| 2. Dissolved gases, vapors, odors | Bilayer lipid or hydrophobic membrane | In series with 1. |
| | Inert metal electrode | amperometric |
| | Enzyme(s) | Amperometric or potentiometric |
| | Antibody, selective receptor | Amperometric or potentiometric or impedance, piezoelectric, optical |
| 3. Substrates | Enzyme(s) | Amperometric or potentiometric in series with 1. or 2. or metal or carbon electrode, conductometric, piezoelectric, optical, calorimetric |
| | Whole cells | As above |
| | Membrane receptors | As above |
| | Plant or animal tissue | As above |
| 4. Antibody / antigen | Antigen/antibody oligonucleotide duplex, aptamer | Amperometric, potentiometric or impedimetric, piezoelectric, optical, surface plasmon resonance |
| | Enzyme labelled | In series with 3. |
| | Chemiluminescent or fluorescent labelled | optical |
| 5. Various proteins and low molecular weight substrates, ions | Specific ligands | As 4. |
| | Protein receptors and channels | |
| | Enzyme labelled | |

| | | |
|--|----------------------|--|
| | Fluorescent labelled | |
|--|----------------------|--|

1.2.1 Measurement Techniques

In an electrochemical sensor, the transducer part serves to transfer the signal from the output domain of the recognition system to the electrical domain. It includes bioreceptor and an electrical interface for all the electrochemical sensors, but the acquisition type of electrical signal can be varied shown in Table 1-2.

Table 1-2 Measurement techniques in electrochemical sensors[7]

| Measurement type | Transducer | Transducer analyte |
|---------------------------------|---|---|
| 1. Potentiometric | Ion-selective electrode (ISE) | K^+ , Cl^- , Ca^{2+} , F^- |
| | glass electrode | H^+ , Na^+ , |
| | Gas electrode | CO_2 , NH_3 |
| | Metal electrode | Redox species |
| 2. Amperometric | Metal or carbon electrode | O_2 , sugars, alcohols. |
| | Chemically modified electrodes | Sugars, alcohols, phenols, oligonucleotides |
| 3. Conductometric, impedimetric | Interdigitated electrodes, metal electrode | Urea, charged species, oligonucleotides |
| 4. Ion charge or field effect | Ion-selective field effect transistor (ISFET), enzyme FET (ENFET) | H^+ , K^+ ... |

1.2.2 Immobilization of a biological recognition element

Immobilization of recognition element is an essential feature in designing the biorecognition part of biosensors. Various immobilization strategies can be envisioned: adsorption, covalence, entrapment, cross-linking or affinity (Figure 1-3).. A seen in figure 1-3, E is the biorecognition (selective) element which can have a variety of bonding mechanisms depending on the application and the nature of its molecule.

Adsorption is the adhesion of atom, ions or molecules from a gas, liquid or dissolved solid to a surface. A covalent bond, also called a molecular bond, is a chemical bond that involves the sharing of electron pairs between atoms.

In entrapment method, the enzyme is trapped in insoluble beads or microspheres, such as calcium alginate beads. However, these insoluble substances hinder the arrival of the substrate and the exit of products. On the other hand, in the Cross-linkage method enzyme molecules are covalently bonded to each other to create a matrix consisting of the almost only enzyme. The reaction ensures that the binding site does not cover the enzyme's active site.

Table 1-3 presents the main advantages and drawbacks of each immobilization method.

Table 1-3 Comparison of immobilization techniques[8]

| | Binding nature | Advantages | Drawbacks |
|-------------------|---|--|--|
| Adsorption | Weak bonds | <ul style="list-style-type: none"> Simple and easy Limited loss of enzyme activity | <ul style="list-style-type: none"> Desorption Non-specific adsorption |
| Covalent coupling | Chemical binding between functional groups of the enzyme and those on the support | <ul style="list-style-type: none"> No diffusion barrier Stable Short response time High enzyme activity loss | <ul style="list-style-type: none"> Matrix not regenerable Coupling with a toxic product |
| Entrapment | Incorporation of the enzyme within a gel or polymer | <ul style="list-style-type: none"> No chemical reaction between the monomer and the enzyme that could affect the activity Several types of the enzymes can | <ul style="list-style-type: none"> Diffusion barrier Enzyme leakage High concentration of monomer and enzyme needed for electropolymerization |

| | | | |
|---------------|---|--|---|
| | | be immobilized within the same polymer | |
| Cross-linking | Bond between enzyme/cross-linker (e.g. glutaraldehyde)/inert molecule (e.g. BSA) | <ul style="list-style-type: none"> simple | <ul style="list-style-type: none"> High enzyme activity loss |
| Affinity | Affinity bonds between a functional group (e.g., avidin) on a support and affinity tag (e.g., biotin) on a protein sequence | <ul style="list-style-type: none"> Controlled and oriented immobilization | <ul style="list-style-type: none"> The need of the presence of specific groups of the enzyme (e.g., His, biotin) |

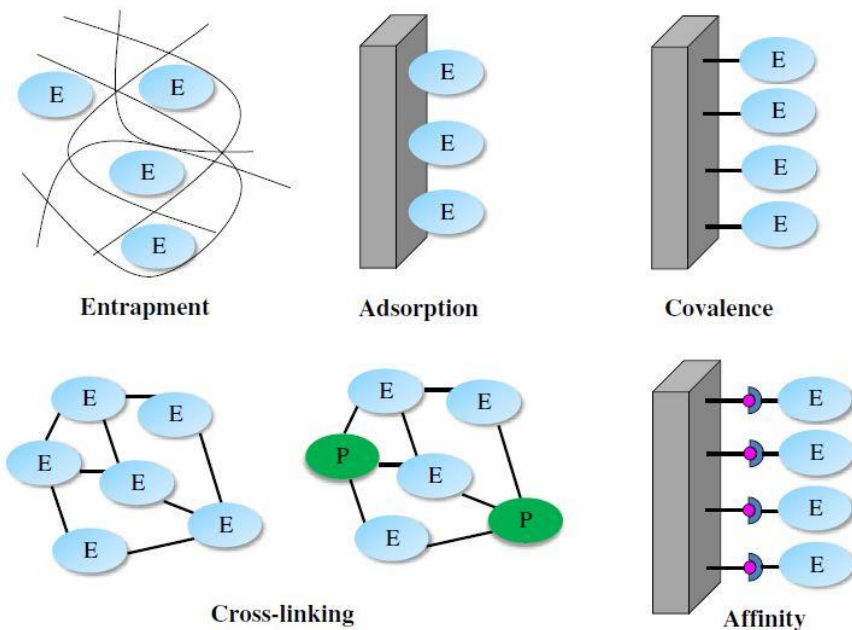


Figure 1-3 Schematic of Immobilization techniques[8]

1.3 Ion-selective sensor

An ion-selective electrode (ISE), also known as a specific ion electrode (SIE), is a transducer that converts the activity of a specific ion in an electrolyte into an electrical

potential or electromotive force(EMF). Based on Nernst equation The voltage is dependent on the logarithm of the ionic activity.Ion-selective electrodes are used in and biochemical research, analytical chemistry where measurements of ionic concentration in an aqueous solution are required. Figure 1-4 shows a schematic of an ion selective sensor. In this sensor, two different half-cell reaction happens at the metal-electrolyte interface. One of the half-cell reaction occurs in electrolyte medium separated from sample solution with ion selective membrane (ISM) therefore this half-cell reaction is representing the activity of the targeted ion, which its selective membrane has been used, and the other one measure the activity of all the ions existed in the sample solution.

Based on Nernst equation, the potential difference between these two-half-cell reactions is correlated to the effective concentration of targeted ions which its selective membrane has been used.

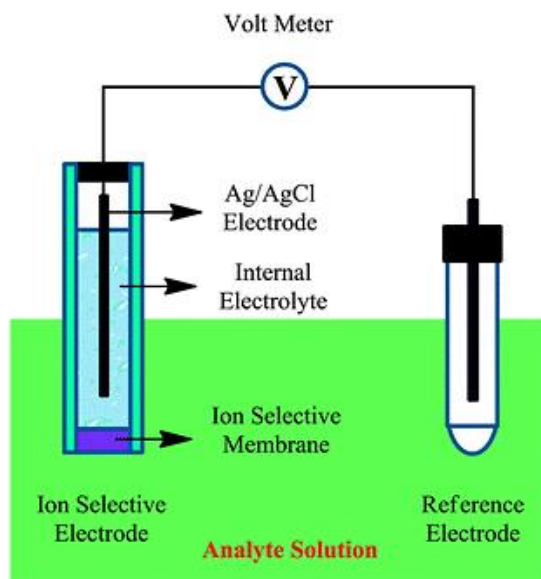


Figure 1-4 Schematic of a macroscale ISE

1.3.1 Reference electrode

A reference electrode has a stable and well-known half-cell electrode potential. The stability of the reference electrode potential commonly reached by employing a redox system with constant (buffered or saturated) concentrations of each participant of the redox reaction. The reference electrodes are commonly used as a half cell to build an electrochemical cell which allows the potential of the other half-cell to be determined. A silver chloride electrode is this type of reference electrode, and it is commonly used in electrochemical measurements. This electrode functions as a redox electrode where the equilibrium is between the silver metal (Ag) and its salt — silver chloride. Recently, solid-state Ag/AgCl planar microelectrodes have shown their significance in microfluidic applications by due to their potential stability and high compatibility.

1.3.2 Ion-Selective Membrane (ISM)

According to the nature of the binding sites, the membranes can be classified as membranes containing fixed sites or membranes containing mobile ion-exchangers or ionophores (carriers). The binding sites are incorporated into the membrane matrix, which determines the internal polarity, lipophilicity, transport and other mechanical properties of the membrane.

There are three main types of ion-selective membranes used in liquid systems:

- 1) Glass membrane electrodes are formed from particular ionically conducting glass. By altering the composition and constituents of the glass, changes can be made to selectivity, chemical resistance, response time, and impedance. The most common glass membrane ion selective electrode is the pH electrode.
- 2) Crystalline or solid state membrane electrodes are made from relatively insoluble ionically conducting inorganic salts. These are available in homogeneous and

heterogeneous forms. They have good selectivity since only ions which can introduce themselves into the crystal lattice can interfere. Examples include the fluoride electrode which uses a doped LaF₃ crystal and the chloride electrode which uses silver chloride powder.

3) Polymer membrane electrodes are based on organic polymer membranes (usually PVC) which contain various ion-exchange ionophores incorporated into an inert matrix. These are used in electrodes to measure ions such as potassium, calcium, and nitrate.

We used the polymeric membrane for measuring the concentration of potassium in the first part of the study. While there are many types of ISM, we decided to invest on ion-exchange resins which are based on special organic polymer membranes. These sensors are the most widespread type of ion-specific electrode. Usage of specific ionophores allows preparation of selective electrodes for tens of different ions, both single-atom or multi-atom.

Preparation of ISM is well-known subject in polymer industries, and their recipes are available online. In this work, our focus is to find and to develop the best ISMs for blood electrolyte panel monitoring that requires trials of different recipes while investigating their sensor characteristics such as sensitivity, selectivity, response time[9],[10][11][12] and their biocompatibility.

Typical membrane components are as follows:

- a) Ionophore (electrode component)
- b) Polymeric Substance
- c) Plasticizer-key role in sensitivity
- d) Neutral Additives-effective in selectivity

It is important to mention that ionophore is the most critical component of ion selective membrane which transports a targeted ion across the membrane.

1.3.3 Nernst Equation

The theory of potentiometric sensors is based on Nicolskii-Eisenman formalism (4) which derived from Nernst equation.

$$E_{Cell} = E_0_{Cell} - (RT/zF) \ln (a_i (I)) \quad (4)$$

Where,

$a_i (I)$ is the primary ion activity in the sample.

E_0_{Cell} is the standard cell potential,

R is the universal gas constant,

T is the temperature in kelvins,

F is the Faraday constant,

Z is the number of moles of electron transferred in cell reaction or half-reaction.

The Nernst equation is easily derived from the standard changes in the Gibbs free energy associated with an electrochemical transformation. For any electrochemical reduction, standard thermodynamics says that the actual free energy change, ΔG related to the free energy change under standard conditions ΔG_0 ,

$$\Delta G = \Delta G_0 - RT \ln Q \quad (5)$$

Where Q is the reaction quotient and is a function of the activities of the chemical species involved in the reaction.

The electrochemical potential E associated with an electrochemical reaction is defined as the decrease in Gibbs free energy per coulomb of charge transfer, which leads to the relationship

$$\Delta G = -ZFE \quad (6)$$

For a complete electrochemical reaction (full cell), the equation can also be written as:

$$E_{\text{Cell}} = E_{0\text{Cell}} - \left(\frac{RT}{zF} \right) \ln(Q) \quad (7)$$

1.4 Electro impedance spectroscopy

Electrical resistance is the ability of a circuit element to resist the flow of electrical current. Ohm's law (Equation below) defines resistance in terms of the ratio between voltage, E , and current, I .

$$R \equiv \frac{E}{I} \quad (8)$$

However, in reality, circuit elements exhibit a much more complicated behavior where the simple concept of resistance cannot explain, and in its place, impedance, a more general circuit parameter has been used. Like resistance in DC, impedance is a measure of the ability of a circuit to resist the flow of electrical current in AC, but unlike DC resistance it is not simplified. Electrochemical impedance should be measured by applying an AC potential to an electrochemical cell and then measuring the current through the cell. Electrochemical impedance is typically measured using a small excitation signal. This is done so that the cell's response is pseudo-linear. In a linear (or pseudo-linear) system, the current response to a sinusoidal potential will be a sinusoid at the same frequency but shifted in phase.

The excitation signal, expressed as a function of time, has the form

$$E_t = E_0 \sin \omega t \quad (9)$$

where E_t is the potential at time t ,

E_0 is the amplitude of the signal,

ω is the radial frequency.

The relationship between radial frequency ω (radians/second) and frequency f (Hz) is:

$$\omega = 2\pi f \quad (10)$$

In a linear system, the response signal, I_t , is shifted in phase (ϕ) and has a different amplitude, I_0 .

$$I_t = I_0 \sin(\omega t + \phi) \quad (11)$$

An expression analogous to Ohm's Law allows us to calculate the impedance of the system as:

$$Z = \frac{E_t}{I_t} = \frac{E_0 \sin \omega t}{I_0 \sin(\omega t + \phi)} = Z_0 \frac{\sin \omega t}{\sin(\omega t + \phi)} \quad (12)$$

With Euler's relationship,

$$\exp(j\phi) = \cos \phi + j \sin \phi \quad (13)$$

The impedance can be represented as a complex number,

$$Z(\omega) = Z_0 \exp(j\phi) = Z_0(\cos \phi + j \sin \phi) \quad (14)$$

One of the plots used for analysis of the EIS data is a Nyquist plot. In equation 14, $Z(\omega)$ is a complex number, therefore, a plot which the x-axis is the real part and the imaginary part is plotted on the y-axis is a Nyquist plot. On the Nyquist plot, the impedance can be represented as a vector (arrow) of length $|Z|$. The angle between this vector and the x-axis, commonly called the "phase angle," is ϕ ($=\arg Z$).

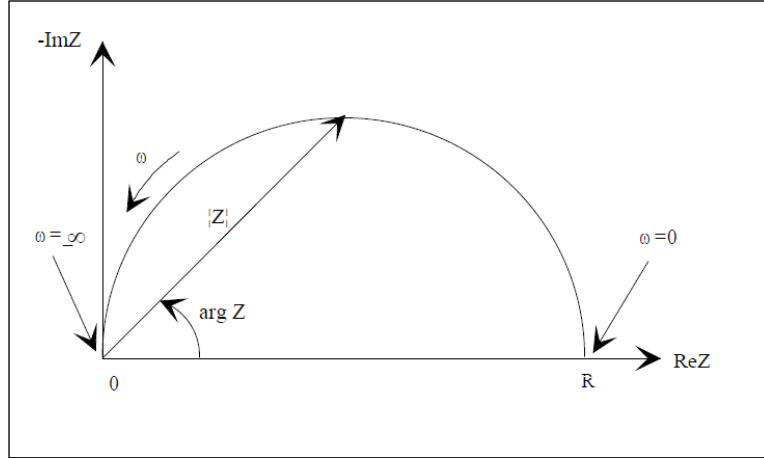


Figure 1-5 Nyquist Plot with impedance Vector[13]

Nyquist plots have one major shortcoming, and it is the lack of frequency data.

Another popular presentation method is the Bode plot. The impedance is plotted with log frequency on the x-axis and both the absolute values of the impedance ($|Z|=Z_0$) and the phase-shift on the y-axis.

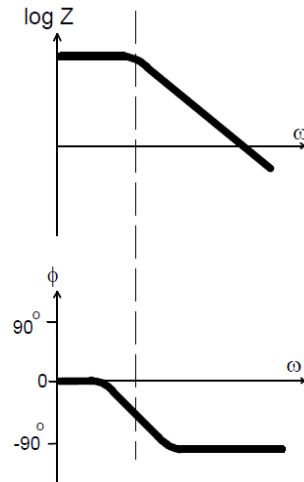


Figure 1-6 Bode plot with one time constant[13]

To analyze EIS data of an electrochemical cell, an equivalent electrical circuit model of the cell should be predicted and be developed. The elements of the equivalent

electrical circuit can be common electrical elements like capacitors, resistors, and inductors. the elements in the equivalent model should be based on the physical electrochemistry of the electrochemical cell.

These physical electrochemistry phenomena are, but not limited to electrolyte resistance, double layer capacitance, polarization resistance, charge transfer resistance, adsorption capacitance and diffusion elements like Warburg impedance.

1.5 Ionic Liquids

Ionic liquids (ILs) may be described as compounds composed entirely of ions that are liquid at a temperature less than 100°C. Ionic liquids have many advantages such as negligible vapor pressure, excellent thermal and chemical stability, high ionic conductivity, wide electrochemical potential windows, good solubility and high synthetic flexibility makes them a miraculous solvent for biological systems[14]. Due to their inimitable properties and a large variety of applications, they have been widely used in enzyme catalysis and protein stability and separation[15].

There are some significant advantages of ILs as compared to water and other aqueous electrolytes. ILs have greater stability at elevated temperatures, are liquid over a much wider temperature range, have tunable physical properties and have selective solubility and selective extractability for various organic compounds, metal ions, and biological molecules[16].

Ionic liquids are not simple liquids. Their ions are generally asymmetric, with delocalized electrostatic charges[17]. The effect of the molecular structure of ionic liquids on their properties such as thermal properties (including the melting point, heat capacity, thermal stability) solubility, viscosity, surface tension, diffusivity, and electrical conductivity has been studied [18], [19].

The molecular forces and interactions of ionic liquids are much more complicated than those of conventional classical salts[18]. Ionic liquids are a mixture of free ions and hydrogen-bonded ionic supramolecular structures[18]. The notable characteristics of ILs are primarily due to their ionic nature. The combination of strong coulombic interactions and weak directional interactions (including hydrogen bonding interactions, cation- π interactions, van der Waals inductive and dispersion interactions) may induce the formation of nano-scale structures in ILs and IL-solvent or IL-solute [18].

The table 1-4 shows the most common anions and cations that are employed in the synthesis of ILs.

Table 1-4 Common anions and cations in ILs[20]

| Cations | Anions |
|---------|--------|
| | |
| | |
| | |
| | |
| | |
| | |
| | |

Chapter 2

Integration of a reconfigurable electrochemical sensor into a digital microfluidic platform

2.1 Literature summary & motivation

Human blood contains many types of ions that regulate essential physiological functions. It has been reported that tracking and monitoring the electrolyte profile of a patient may allow early diagnosis of diseases and efficient prognosis[21]. In addition, electrolyte profile would provide valuable information about a patient's condition in places such as emergency rooms. Although disposable sensors have been developed and some of them are commercially available, they can measure only one type of analytes. To measure multiple analytes with one sensor platform an assay of different types of sensors needs to be integrated, which is not readily achievable due to incompatible structures among sensors. Moreover, combining sensor elements with liquid sample handling means is not a simple task.

Droplet-based microfluidics (a.k.a. digital microfluidics; DMF) have drawn significant attention in the field of lab-on-a-chip (LOC) technology. Compartmentalization of fluid in DMF allows many advantageous features, such as reduced dispersion of reactants, enhanced mixing by recirculation, and fast molecular transport due to high interfacial area-to-volume ratio. Electrowetting-on-dielectric (EWOD) is one of the mainstream principles that enable DMF. The superior features of EWOD DMF include complete flexibility and simplicity in individual and independent use of each droplet as a tiny and convenient reaction vessel and a fluid carrier in a microfluidic system. Furthermore, EWOD DMF has user-definable (or reconfigurable) fluidic pathways and multiplexing capability, which makes it highly suitable for a LOC platform for analytic processes that require complex combinations of liquid handling, as well as accurate control of volume and flow rate [22].

To build a complete LOC to perform chemical and biological analysis, however, integration of liquid handling units and analytic units such as detectors and sensors must be done. There have been efforts to integrate optical sensors in digital microfluidics [23], but they are not yet portable nor cost-effective systems. With the improvements in solid-state microelectrochemical sensors and the growth of bio-electrochemical sensors in the past two decades [24] [25], electrochemical analysis has once again shown the importance of their simplicity and ease of fabrication [6]. The manufacturing methods of electrochemical sensors [26] and EWOD DMF are fundamentally similar, which makes them inherently compatible with each other [27] [26]. Recently, several different types of electrochemical sensors were integrated into EWOD DMF platforms. Amperometric sensing using gold as electrodes were implemented to detect ferrocene methanol and dopamine in EWOD DMF[28]. Capacitive sensors were integrated into EWOD DMF and managed to detect different concentrations of cryptosporidium in sample droplets[29].

Among all electrochemical sensors, potentiometric sensors have many advantages such as rapid response, reproducibility, and simplicity of measurements [30]. However their integration with LOCs has been challenging due to rapid dissolution of the silver chloride (AgCl) layer of the reference electrode in the sample solution, hence a short lifetime of a sensor [31].

In this study, therefore, we report the integration of ion-selective potentiometric sensors into the EWOD DMF platform addressing challenges mentioned above. As the proof-of-concept model system, polymer-based potassium selective electrodes are fabricated. To complete the sensor fabrication, the liquid handling capability of EWOD DMF is actively utilized. We refer to this approach as "on-chip fabrication of sensors." This new method of fabrication allows not only seamlessly integrating sensors with the sample preparation platform, but also reconfiguring sensors on demand without any

interruption or the disassembling of the device. Moreover, this method ensures the lifetime of reference electrodes in sensors by redepositing the Ag/AgCl layer on-chip. This paper focuses on the demonstration of the proposed on-chip fabrication of sensor array. The potassium ion concentration measurement through a fabricated sensor will be compared with ion-selective electrodes theory.

2.2 Materials & Methods

2.2.1 Materials

A gold (Au, 1000 Å)/chromium (Cr, 100 Å) coated glass wafer was used to fabricate the integrated device. Metal layers (Au/Cr) were used for the seed layer of ion-selective electrodes as well as for EWOD electrodes. S1813 (MICROPOSIT) was used as the photoresist for the photolithography and etching mask layers in different stages of fabrication. SU-8 2005 (Micro-Chem) was used as the dielectric layer of EWOD device. Teflon AF1600S (Du Pont) powder dissolved in the Fluorinert FC-40 (Sigma-Aldrich) for creating a 4wt% solution which was used to spin coat the hydrophobic layer of EWOD device. 1025 RTU @4.5 TROY/GALLON (TECHNIC INC) was used as the silver (Ag) electroplating solution. Hydrochloric acid (HCl) analytical reagent grade was used for the formation of the AgCl layer.

For the potassium ion-selective membrane solution, 1 wt % of potassium ionophore I, 0.5 wt %, potassium tetrakis (4-chlorophenyl) borate, 49.5 wt % bis (2-ethylhexyl) sebacate, and 49 wt % polyvinyl chloride (PVC) were dissolved in Tetrahydrofuran (THF-T397-4). All materials for the membrane solution were purchased from Sigma-Aldrich.

Different molarities of the potassium chloride (KCl) solution (1µM-1M) were prepared by the serial dilution of 1 M stock solution. The stock solution was prepared by dissolving KCl powder (Sigma-Aldrich) in deionized water.

Technics Micro-RIE Series 800 Plasma System was used to selectively etch and modify the surface properties of the Teflon layer. Electromotive force (EMF) was measured with a high input impedance ($10^{12}\Omega$) by HP 34401A Multimeter at room temperature (21°C) in the electrochemical cell fabricated on the chip.

2.2.2 Sensor design and configuration of the EWOD-electrochemical cell

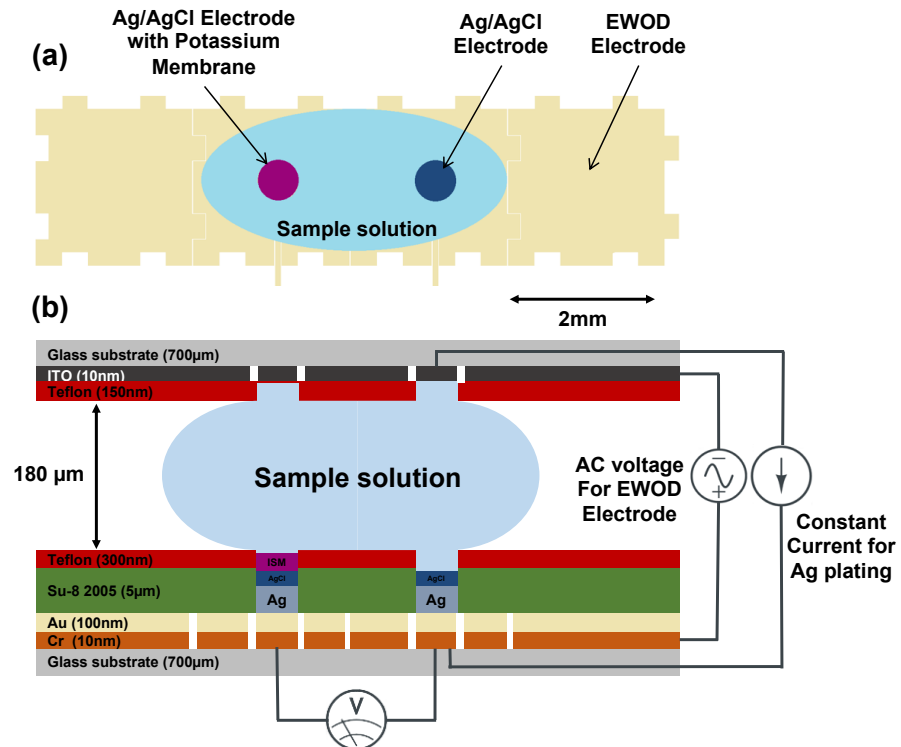


Figure 2-1 Schematics of an electrochemical cell integrated with EWOD electrodes.

(a) The top view, and (b) the side view with electrical circuits for EWOD DMF operation, electroplating, and potentiometric measurement.

Figure 2-1 (b) shows the configuration of the EWOD electrochemical cell. The top plate is a glass substrate coated with indium tin oxide (ITO) layer that serves as a ground

electrode for EWOD operation as well as a cathode electrode for electroplating of Ag. The bottom chip contains a patterned gold layer that serves as EWOD electrodes and the seed layer of potentiometric sensor electrodes. Although using Au electrodes as non-corroding metal is common to cyclic voltammetric and amperometric sensors, a potentiometric electrochemical sensor requires a redox couple to maintain a stable potential and to provide accurate voltage measurement during voltage measurements. An Ag/AgCl reference electrode that contains saturated standard solution can provide long-term stability for electrochemical sensors but integrating such reference electrode in a LOC system results in a much more expensive and complicated system and does not fit for portable devices [32]. The significant improvement in the fabrication of solid-state Ag/AgCl electrodes through electroplating and chemical anodization, where the electroplated forms a quasi-bulk phase[31], allows for the subsequent formation of a much thicker silver chloride while having a much rougher surface. This leads a larger and electrochemically active surface area with higher stability where electromotive force, i.e., voltage, measurements can be achieved [31]. However, due to the short lifetime of these electrodes, little research has been done to integrate Ag/AgCl electrodes with portable and reusable LOC devices. To eliminate the short lifetime problem, we chose to design our sensor platform in which Ag/AgCl electrodes are fabricated on demand using EWOD DMF liquid handling capability rather than to have a platform containing ready-made sensor elements.

To dispense and locate droplets of required reagents, six reservoirs where each reagent is held and dispensed as a ~650 nL droplet, and 45 EWOD actuating electrodes ($2 \times 2 \text{ mm}^2$ each) are placed in the platform. Entire platform layout can be found in section 2.2.4. As for the potassium selective sensor array, we designed four electrochemical cells where the sensor electrode (circular shape with $400 \mu\text{m}$ diameter) is

placed in the middle of an EWOD electrode. The ratio between an EWOD actuating electrode and the sensor electrode (i.e., the hydrophilic-to-hydrophobic ratio) plays a significant role in the movability of the droplets in the sensing sites [26]. We chose 3.1% as our ratio to ensure the maximum level of movability while having enough hydrophilic area for pinching off the ion-selective membrane solution during the on-chip fabrication of sensors of which details are discussed in the next section.

2.2.3 EWOD Chip Fabrication

In this section, the fabrication steps of an EWOD DMF chip are detailed, while the next section will address the on-chip fabrication steps of the sensor electrodes in the EWOD DMF chip. Figure 2-2 illustrates the fabrication of the bottom chip of an EWOD DMF device. The electrodes of the EWOD device and the sensor electrode were patterned by standard photolithography followed by wet chemical etching of the Au/Cr layer. SU-8 2005 (a negative photoresist) was then spin coated and photolithographed to form a dielectric layer over the EWOD electrodes with a thickness of 5 μm . Afterward, a Teflon layer (~ 300 nm) was spin coated and baked to form a hydrophobic surface. To etch the Teflon layer on top of the sensor electrode, we had to mask the desired Teflon layer. To do so, we treated the Teflon surface for 5 seconds with 140 W of power at an argon rate of 30 sccm by reactive ion etching (RIE) to make the surface ready for the spin coat of S1813, a positive photoresist needed for forming the RIE etching mask. After selectively etching the Teflon layer over the sensor electrodes for 230 seconds by RIE with the power of 160 W at the same argon rate, the layer was exposed to UV light (flood exposure) to weaken the remaining photoresist and was removed by dissolving it in an acetone solution. Finally, after placing the chip in an oven at 200 $^{\circ}\text{C}$ for one hour, the Teflon surface recovered its hydrophobic properties and got ready for EWOD operation. As for the top chip of an EWOD DMF shown in Figure 2-1(b), the fabrication started with

patterning ITO layer using photolithography method. S1813 was used as photoresist and MF-319 as developer solution. The photoresist patterning process followed by wet etching in ITO etchant (8:1:15 vol % HCl: HNO₃: H₂O) for 165 seconds. After dehydrating the patterned ITO wafer, the same process mentioned above was used to pattern Teflon selectively to creates the openings for ITO electrode to work as the cathode at the time of electroplating while keeping Teflon layer on other areas which function as the ground electrode for operating EWOD DMF.

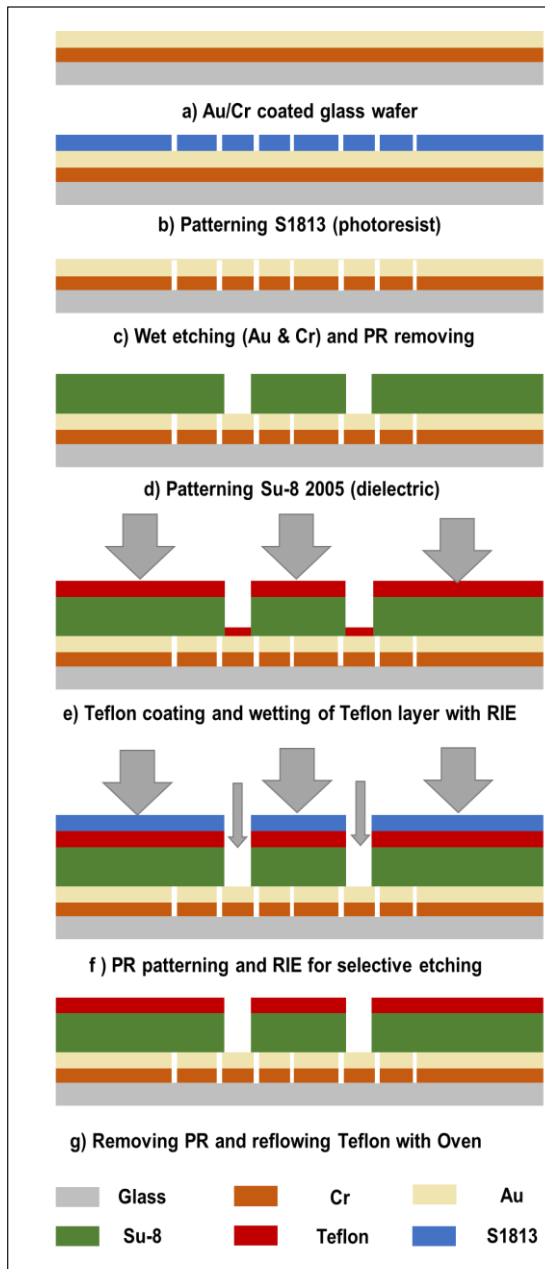


Figure 2-2 Fabrication process of the bottom chip of an EWOD DMF device.

2.2.3.1 EWOD Chip Fabrication reactive ion etching

In the EWOD fabrication, reactive ion etching (RIE) was used shown in Fig 2-2 (f). Reactive ion etching is a kind of dry etching method. RIE uses chemically reactive plasma to remove material deposited on wafers. Its etch rate is dependent on the gas, operating power and deposited material and structure.

Since Teflon used in spin coating step for EWOD chip fabrication is a customized solution, a characterization study of dry etching of Teflon layer was necessary for finding the exact etch rate. Three glass wafers with Teflon opening was prepared via spin coating and selective taping for measuring the thickness via profilometer at a different time of etching via RIE as shown in the figure below.

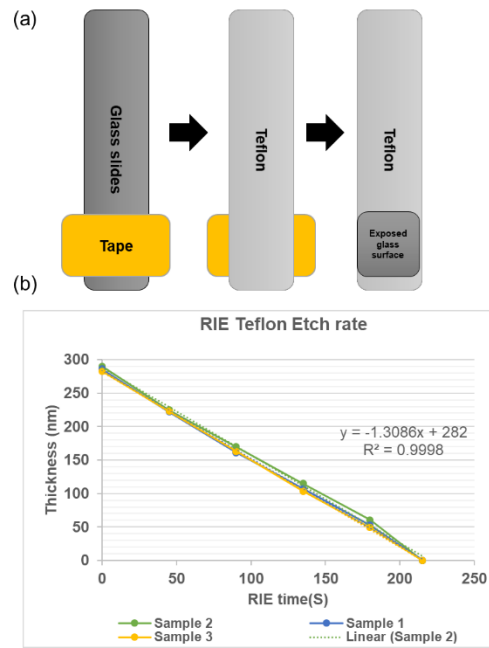


Figure 2-3 Characterization of the etching rate of the RIE of Teflon.

(a) Sample preparation method for RIE characterization. (b) Thickness Vs. Time.

The calculated etch rate form Figure 2-3(b) is 1.3 nm/s for RIE with the operating condition of 160 Watts and 30sccm argon gas.

2.2.3.2 EWOD Chip Fabrication-SU-8 mask & electroplating

During the electroplating of Ag layer, higher thickness of electroplated silver was observed on the edges of sensor electrode which result in a non-uniform thickness of sensor surface and eventually failure in AgCl oxidation process and even formation of the membrane. This phenomenon shown in Figure 2-4 can create an impediment for droplet moveability over the sensor in EWOD platform and, moreover, affect the stability of response of sensors.

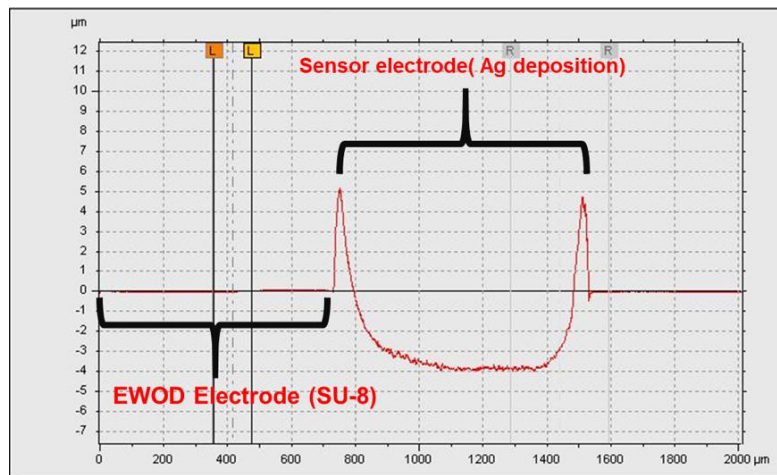


Figure 2-4 A scan of sensor electrode integrated with EWOD electrode

This behavior exists because the surface of a conductor has constant potential, and the electric field must be perpendicular to the surface at any point on the surface. So, if the geometry of a conductor is very sharp, the electric field lines will diverge at large angles respective to each other creates a large field gradient at that sharp edge.

For better understanding, consider a charged conductor made from two spheres of radii R_1 and R_2 , connected with a conducting wire. Assume that $R_1 < R_2$, and that the

spheres are far apart so that effects of electrostatic interactions between the spheres can be neglected. Then, the surface charge density, the quantity that describes how crowded the charges are, is higher at the smaller sphere. since this system is a conductor, its surface is an equipotential. Therefore, the electric potential on the surface of two spheres is the same, $V_1 = V_2$ which implies that

$$\frac{q_1}{R_1} = \frac{q_2}{R_2} \rightarrow \frac{q_1}{q_2} = \frac{R_1}{R_2} < 1 \quad (15)$$

i.e., that most of the charge is in the bigger sphere. However, the ratio of the surface charge densities behaves the opposite way as shown below

$$\frac{\sigma_1}{\sigma_2} = \frac{\frac{q_1}{4\pi R_1^2}}{\frac{q_2}{4\pi R_2^2}} \rightarrow \frac{q_1 R_2^2}{q_2 R_1^2} = \frac{R_2}{R_1} > 1 \quad (16)$$

This proves that the surface charge density of the smaller sphere is more significant compared to bigger one. Knowing that in electroplating reaction charges on the surface of the conductor are used for deposition of the free ion in the electrolyte solution. Therefore the edges with higher charge density result in higher deposition rate while electroplating which results in non-uniform deposition layer over the surface. The elimination of edge effect through modification of Su8 layer has been shown in the figure 2-5.

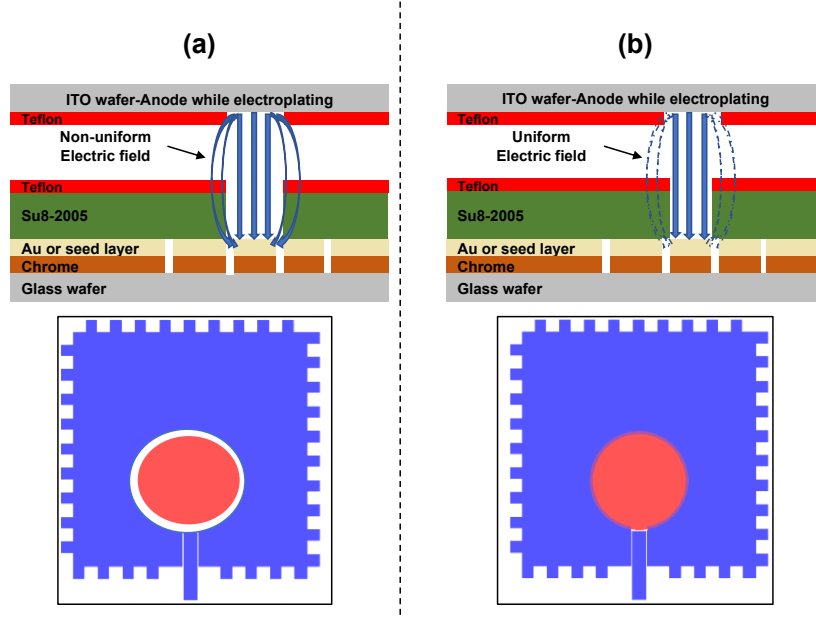


Figure 2-5 (a) Initial sensor design (sensor edges are open to the electric field), (b) enhanced design (Su8 covering the edges of sensor electrode)

After changing the design of Su8 mask in EWOD fabrication, another electroplating was conducted to confirm the uniformity of electroplated silver on Au seed layer in EWOD chips, the figure below shows before and after of electroplating of the redesigned integrated sensor.

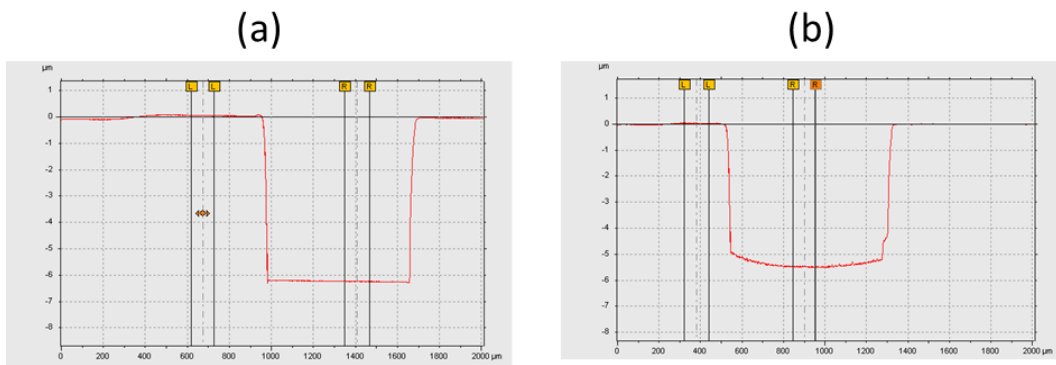


Figure 2-6 Electroplating thickness characterization;(a) before electroplating, and (b) after electroplating.

2.2.3.3 On-chip fabrication & calibration of potassium ion selective sensor

After loading reagents solutions to designate reservoirs as shown in Figure 2-7, the top chip was placed to complete EWOD DMF device. Figure 2-7 illustrates steps of on-chip sensor fabrication. Firstly, a droplet (~650 nL) of Ag plating solution was dispensed from the reservoir and brought over the sensor site by EWOD microfluidic actuation (Step 1). Electroplating was driven at 12 mA/cm^2 for 300 seconds. To avoid the depletion of silver ion, silver plating solution droplets were replenished during electroplating as needed. Similarly, a droplet of 0.1 M HCl solution was dispensed from the designated reservoir and brought over to the Ag-plated electrodes (Step 2) and applied to the surface for 45 seconds to form an AgCl layer.

It is worth mentioning that since the Ag/AgCl reference electrode works as a redox electrode and the equilibrium is between Ag layer and AgCl layer, the thickness of the Ag may affect the lifetime of the sensor, but it has nothing to do with the stability of potential measurement during sensing.

Lastly, a droplet was dispensed from the membrane solution reservoir and brought over to a sensor electrode to form the layer of potassium-selective membrane (Step 3). Due to the wettability contrast, the membrane solution was pinched-off at the hydrophilic opening of the sensor electrode and left a tiny portion of it on the sensor electrode (Figure 2-9). After the evaporation of THF, the solvent of the membrane solution, a thin layer of the potassium-selective membrane was formed over one of the sensor electrodes.

Regarding sample preparation, although serial dilution step of the sample solution was proposed for on-chip calibration, in this research, all the solutions required for calibration process was prepared off-chip to avoid any possible errors caused by on-chip serial dilution.

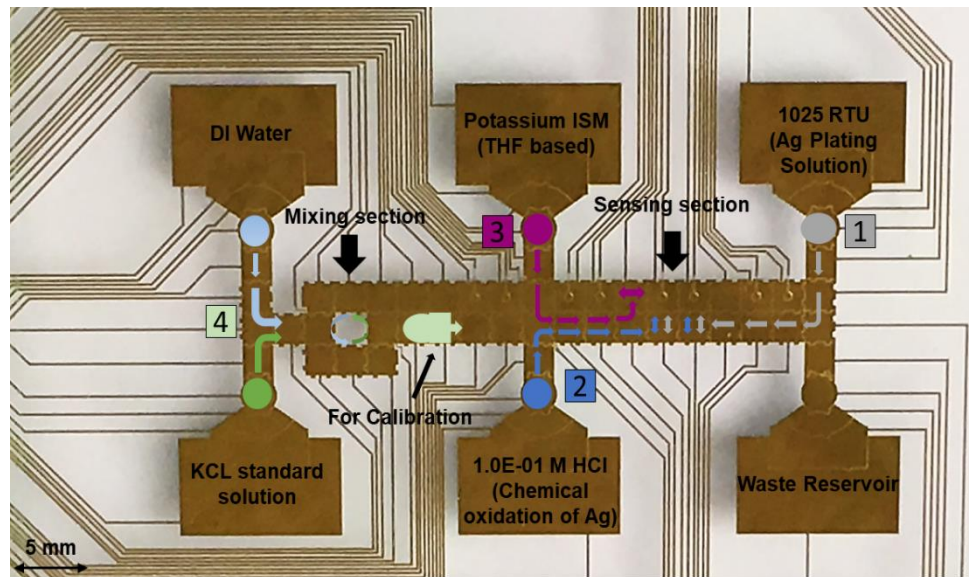


Figure 2-7 On-chip ion-selective electrodes fabrication and calibration procedure.

Step (1) is dispensing a droplet from Ag plating solution reservoir and transporting it to sensor electrode for electroplating Ag on patterned Au as seed layer, Step (2) is chemical oxidation of Ag layer with HCl solution using EWOD electrode for precise manipulations, Step (3) is forming a thin layer of ion-selective membrane on a sensor electrode, and Step (4) is serial dilution for on-chip calibrating of the sensor (this step is proposal only).

2.3 Results and Discussion

2.3.1 On-chip Fabrication of Ag/AgCl reference electrodes

On this DMF platform, the solid Ag/AgCl reference electrodes are fabricated through electroplating followed by chemical oxidation of the electroplated layer. This method requires the sensor electrodes to be exposed to solutions, unlike the EWOD electrode on which a dielectric layer is necessary for charge polarization and changing the surface energy. While we optimized the chip design and fabrication processes, we observed severe edge effect during the on-chip electroplating process. When entire sensor

electrodes were exposed to the plating solution, the edges of electrode experience high electric field densities compare to the center part. This resulted in the much faster Ag deposition rate along the edge of an electrode so that the plated Ag layer became highly non-uniform. This problem was solved by patterning the dielectric layer to cover edges of a sensor electrode. With the optimized design, successful on-chip electroplating of Ag was achieved as shown in Figure 2-8.

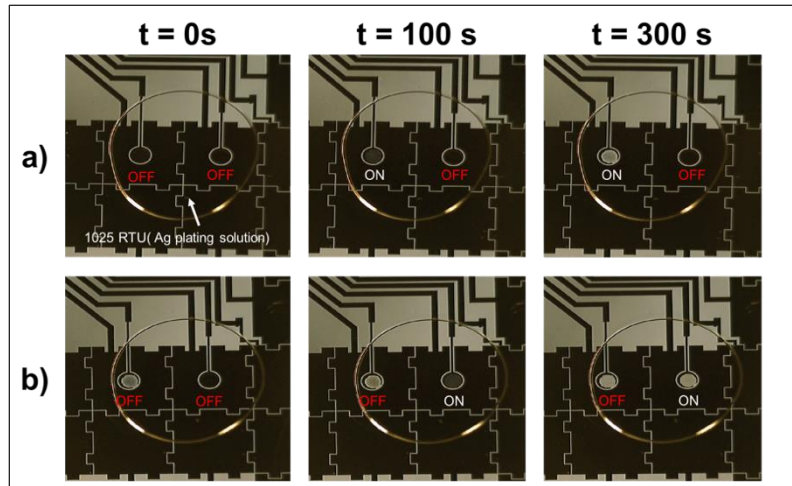


Figure 2-8 On-chip electroplating of Ag demonstration.

(a) Ag deposition on the left sensor electrode, and (b) Ag deposition on the right sensor electrode.

2.3.2 *On-chip formation of Potassium ion selective membrane*

It is important to mention that THF has been used as a solvent for dissolving potassium ion selective membrane (ISM) components, but in this study, it was also used it as a carrier fluid to move the membrane solution on the EWOD DMF platform. THF as an insulating fluid is only movable at low frequencies compared to other liquids[33]. Usually, ISM cocktail components are dissolved in THF with the weight ratio of (1:10), then the mixture poured over the designated area and let the THF evaporate to form a gel-like membrane. However, this ratio makes ISM solution highly viscous and hinders

ISM solution droplet movability in EWOD device significantly. Therefore, the (1:15) ratio has been used to enhance movability and pinching off process shown in Figure 2-9 while compensating the amount of THF evaporated during the on-chip fabrication process.

The thickness of the ISM is correlated to the volume of the pinched-off ISM solution over sensor electrodes, which is controlled by the area and geometry of the hydrophilic opening. Small variations in volume were inevitable, but they resulted in negligible variation in thickness of ISM. This might lead to little changes in response time but had no significant effect on the electromotive force (EMF) measurement at the equilibrium.

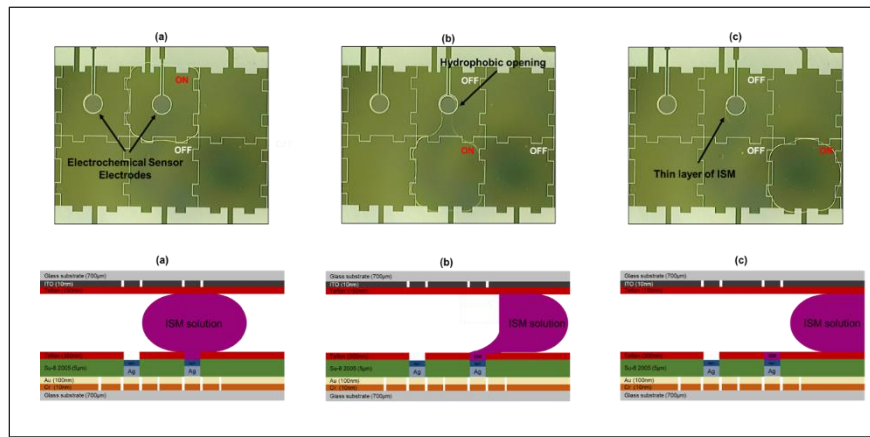


Figure 2-9 Top and side view of ISM solution pinching-off process.

(a) an ISM solution droplet brought over a sensor electrode by EWOD motion, (b) the ISM solution droplet is being driven away from the sensor electrode while a part of ISM solution is wetting the hydrophilic opening over the electrode, and (c) a thin layer of ISM on sensor electrode after the completion of pinch-off and evaporating the solvent(THF).

2.3.3 Calibration

The composition of the potassium ISM solution mentioned in section 2.1 has been outsourced from Sigma Aldrich and has been already tested for measurement of

potassium concentration in whole blood during open-heart surgery [34] and determination of potassium ion concentration in serum [35]. Additionally, selectivity ratio for interfering ions has been reported by the manufacturer (presented in below). As mentioned earlier, we kept the same standard composition as the published specification, but only further diluted it by adding more THF to make ISM solution less viscous. This dilution, however, will not affect the final ISM properties and because THF will be evaporated to form gel-like ISM and the final ISM will have the same composition with the specification. The theory of potentiometric sensors is based on Nicolskii-Eisenman formalism derived from Nernst equation.

$$E_{cell} = E_{0\ cell} - \frac{RT}{ZF} \ln a_i(I) \quad (17)$$

Based on Equation (17) the slope of all the potentiometric ion-selective sensors at room temperature should be equal or close to RT/ZF which is 57-59 mV/log for the case of potassium ion.

Potassium chloride solutions of eight different molarities (10^{-6} – 10^{-1} M) were prepared and dispensed to a sample reservoir one at a time. Then droplets of each molarity were brought over the on-chip fabricated potassium ion-selective electrode, and EMF was measured with a high input impedance ($\sim 10^{12} \Omega$) by HP 34401A Multimeter at room temperature (21°C). This experiment was repeated 3 times to ensure the reproducibility of Data, Activity coefficients of the potassium ion in each sample has been calculated from the concentration of potassium ion, its ionic strength in presence of chloride ion. Table 2-1 lists the data of experiments and Figure 2-10(a) shows the time vs. EMF measurement of different molarity samples. As seen in the figure, EMF output from each sensor is well stabilized within 250 s. To validate the sensor, the slope Nernstian response of the fabricated sensor was compared with the theoretical value. As shown in Figure 2-10 (b), EMF averaged data at $t = 210$ s were plotted to calibrate the

sensor. The plot has a slope of 58 mV/log which is within the acceptable range (57 – 59 mV/log) for a successful potassium ion selective sensor according to the theory of potentiometric sensor.

Table 2-1 Electromotive responses of different molarities of KCl solutions in three experiments @ t=210s.

| Log(a(K+)) | EMF 1 (V) | EMF 2 (V) | EMF 3 (V) | STD (V) | Averaged EMF (V) | STD % |
|------------|------------|------------|------------|----------|------------------|-------------|
| -5.97 | -0.264919 | -0.261124 | -0.27124 | 0.004173 | -0.265761 | 1.570033285 |
| -5.27 | -0.237448 | -0.242827 | -0.240681 | 0.002211 | -0.240318667 | 0.919971495 |
| -4.97 | -0.220589 | -0.222433 | -0.221006 | 0.000713 | -0.2217195 | 0.321802999 |
| -3.97 | -0.172821 | -0.170214 | -0.171135 | 0.000461 | -0.17139 | 0.268685454 |
| -2.98 | -0.104309 | -0.104001 | -0.103959 | 2.1E-05 | -0.104089667 | 0.020174913 |
| -2.02 | -0.046569 | -0.046004 | -0.045969 | 1.75E-05 | -0.046180667 | 0.037894646 |
| -1.36 | -0.0245244 | -0.0225882 | -0.0245529 | 0.000982 | -0.0238885 | 4.112229734 |
| -1.09 | 0.0235425 | 0.0230003 | 0.0232359 | 0.000118 | 0.023259567 | 0.506458275 |

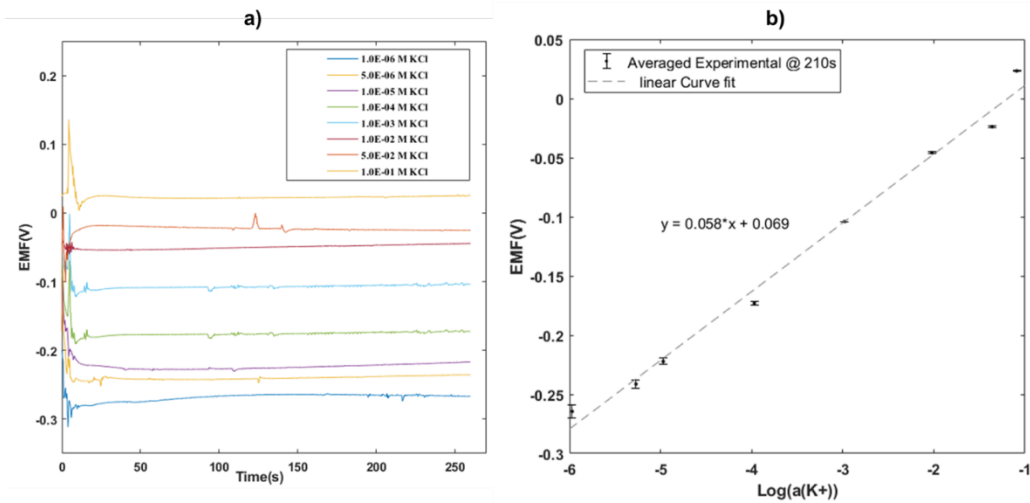


Figure 2-10 EMF responses vs. time and Log(a)

a) Measuring EMF (electromotive force) on EWOD with respect to time, b) Nernstian response to the different molarity of KCl solutions (calibration curve)

For developing an ion selective sensor, it is essential to acquire all the selectivity coefficients for the other ions with the same charge, however, as mentioned above the membrane composition was outsourced from Sigma Aldrich. The Selectivity coefficients $\text{Log}K_{K,M}^{\text{Pot}}$ as obtained by the separate solution method (0.1 M solutions of chlorides) reported by Sigma Aldrich as follows:

$$\text{Log}K_{K,Li}^{\text{Pot}} = -3.98, \text{Log}K_{K,Na}^{\text{Pot}} = -3.56, \text{Log}K_{K,Ca}^{\text{Pot}} = -4.3, \text{Log}K_{K,NH_4}^{\text{Pot}} = -1.81$$

Moreover, the reported Slope of linear regression is $57.5 \pm 0.2 \text{ mV}$ (10^{-1} to 10^{-5} M KCl) which is matched with the experimental data.

2.4 Conclusion & Outlook

The integration of potassium ion selective potentiometric sensor with EWOD microfluidic platforms was investigated experimentally.

An EWOD-electrochemical cell chip is designed, fabricated and used as a microfluidic platform to introduce “on-chip” electroplating and chemical oxidation to fabricate the Ag/AgCl electrodes needed for potentiometric measurements. On-chip fabrication of ion-selective electrode also includes the formation of potassium ion selective membrane over one of the electrodes. Finally, the calibration curve of EMF measurement from fabricated sensors against eight different molarities of KCl solutions was obtained. The slope of 58 mV/dec of the calibration curve was achieved and in a good agreement with the theoretical value. Although more studies needed for determining the static and dynamic characteristics of proposed sensors, this study responds to the primary challenge of the potentiometric sensor by adding lifetime to sensor electrodes while adding a reliable and reproducible analysis unit to lab-on-a-chip devices. The on-chip fabrication of Ag/AgCl showed the possibility of restoring reference electrodes after their lifetime, while the on-chip formation of the ion selective membrane presents a possibility for on-demand fabrication (i.e., reconfiguration) for assessing arbitrary assays using the same platform.

This method of fabrication can pave the path to low cost and compatible home-use sensors with the benefits of EWOD, such as ease of use, automation, and minimal consumption of reagents.

Chapter 3

Simultaneous measurement of K⁺, Na⁺ and Ca²⁺ concentrations in a droplet of a human blood plasma emulated solution

3.1 Motivation

More than 3 million US cases per year, the metabolic syndrome is a cluster of cardiometabolic risk factors associated with increased risk of multiple chronic diseases, including cancer and cardiovascular disease. Among US adults aged 18 years or older, the prevalence of metabolic syndrome increased from 25.3% to 34.2% from the years of 1988–1994 to the years of 2007–2012. Many studies have shown the positive effect of the dietary approaches to stop hypertension. Whelton et al. have demonstrated the dependency of blood pressure on our dietary sodium[36]. Among many assays existed in blood analysis, Lipid panel (LP) and basic metabolic panel (BMP) (Table 3-1 & 3-2) have shown their importance via frequent monitoring for patients suffering from metabolic syndromes such as hypertension and diabetes.

Monitoring basic metabolic panel (BMP) and lipid panel (LP) helps patients and their health provider to plan preventive strategies such as adjusting dietary choices and change of their exercise routine. Also, in another study, Cohn et al. found that patients with the severe mental illness have markedly elevated rates of metabolic disturbances, suggesting that clinicians should screen patients for metabolic disturbance and should track the effects of antipsychotic treatment on metabolic parameters [21]. However, the efficiency of these diets or treatments relies on the capability of frequent screening of BMP's and LP's . The current state of the art BMP testing requires blood sample collection in a lab by a certified phlebotomist and lab analysis by a technician. This process is time-consuming and expensive, and needless to say, uncomfortable for daily

health monitoring. Additionally, this multi-sided process makes it difficult to establish a cohesive database for BMP and LP of the patient's blood.

In this study, we propose a LOC that only needs a droplet(5-7 μ L) of the sample for simultaneous concentration measurement of Ca^{2+} , K^+ and Na^+ with help of an solid state electrochemical potentiometric assay. Fabrication and calibration of potassium selective electrode has been investigated in the last chapter therefore in this chapter we focused on fabrication and calibration of calcium and sodium selective electrode which follows the similar method with potassium ion selective sensor.

After acquiring calibration curve, simultaneous measurement was conducted on an emulated human blood plasma solution for addressing the capability of the solid-state electrochemical assay.

Table 3-1 Serum elements of basic metabolic panel

| Assay | Basic Metabolic Panel (BMP) | | | | | | | |
|-------|-----------------------------|----------------|-----------------|---------------|-------------|--------------|---------------|--------------|
| | Serum Elements | K+ | Na+ | Ca++ | Cl- | Bicarbonate | Glucose | Creatinine |
| Range | 3.5- 5.0 mEq/L | 136- 142 mEq/L | 8.2- 10.2 mg/dL | 96- 106 mEq/L | 21-28 mEq/L | 70-140 mg/dl | 0.6-1.5 mg/dl | 5 - 23 mg/dl |

Table 3-2 Serum elements of Lipid panel

| Assay | | Lipid Panel (LP) | | |
|----------------|--|------------------|-----------------|-----------------|
| Serum Elements | | Cholesterol | Triglycerides | LDL-C |
| Range | | Up to 250 mg/dl | Up to 180 mg/dl | Up to 200 mg/dl |

3.2 Material & Methods

3.2.1 Material

A gold (Au, 1000 Å)/chromium (Cr, 100 Å) coated glass wafer was used to fabricate the integrated device. Metal layers (Au/Cr) were used for the seed layer of ion-selective electrodes as well as for EWOD electrodes. S1813 (MICROPOSIT) was used as the photoresist for the photolithography and etching mask layers in different stages of fabrication. SU-8 2005 (Micro-Chem) was used as the dielectric layer of EWOD device. Teflon AF1600S (Du Pont) powder dissolved in the Fluorinert FC-40 (Sigma-Aldrich) for creating a 4wt% solution which was used to spin coat the hydrophobic layer of EWOD device. 1025 RTU @4.5 TROY/GALLON (TECHNIC INC) was used as the silver (Ag) electroplating solution. Hydrochloric acid (HCl) analytical reagent grade was used for the formation of the AgCl layer.

The composition of the proposed potentiometric assay as follows:

For sodium ion selective membrane

10 wt % of Sodium ionophore I,

0.5 wt %, Sodium tetraphenylborate,

89.5 wt % 2-Nitrophenyl octyl ether,

For calcium ion selective membrane, a membrane cocktail was purchased from Sigma Aldrich with the following composition:

1 wt % of Calcium ionophore IV,

0.022 wt %, of potassium tetrakis (4-chlorophenyl) borate,

4.748 wt % of 2-Nitrophenyl octyl ether,

2.379 wt % of polyvinyl chloride (PVC)

92.78 wt % of Tetrahydrofuran,

Moreover, for the potassium ion-selective membrane solution, 1 wt % of potassium ionophore I, 0.5 wt %, potassium tetrakis (4-chlorophenyl) borate, 49.5 wt % bis (2-ethylhexyl) sebacate, and 49 wt % polyvinyl chloride (PVC) were dissolved in Tetrahydrofuran (THF-T397-4).

For calibration of off-chip sensors, six different molarities of the sodium chloride (NaCl) and calcium chloride (CaCl_2) solutions ($1\mu\text{M}$ - 1M) were prepared by the serial dilution of 1 M stock solution. The stock solutions were prepared by dissolving NaCl and CaCl_2 powders (Sigma-Aldrich) in deionized water.

3.2.2 Fabrication of potentiometric ion selective sensor assay

For the preparation of the ISE assay , firstly, a droplet ($4 \mu\text{L}$) of Ag plating solution was dispensed over the sensor electrode then, electroplating was driven at 12 mA/cm^2 for 300 seconds. To avoid the depletion of silver ion, Ag plating solution droplets were replenished during electroplating as needed. Similarly, a droplet ($4 \mu\text{L}$) of 0.5 M HCl solution was dispensed over the Ag-plated electrodes for 45 seconds to form an AgCl layer. Lastly, a droplet of desired membrane solution was dispensed over one of the electrodes. Figure 3-1 shows the schematic of the final off-chip sensor.

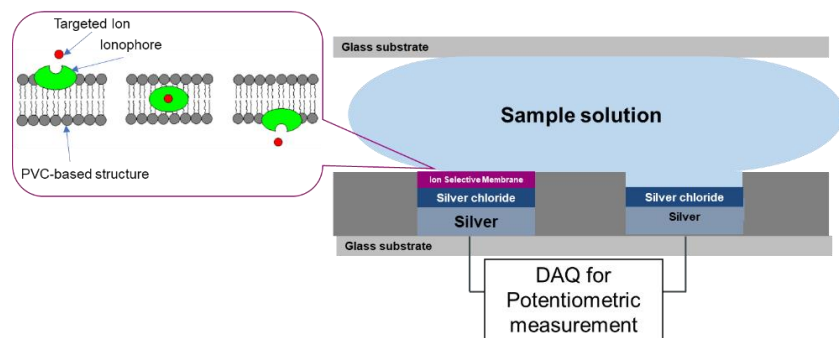


Figure 3-1 Schematic side view of the potentiometric sensor

Since our goal is to integrate these sensors with EWOD platform, a sensing platform was designed in which the electrodes are the same design as intended to use on our EWOD platform.

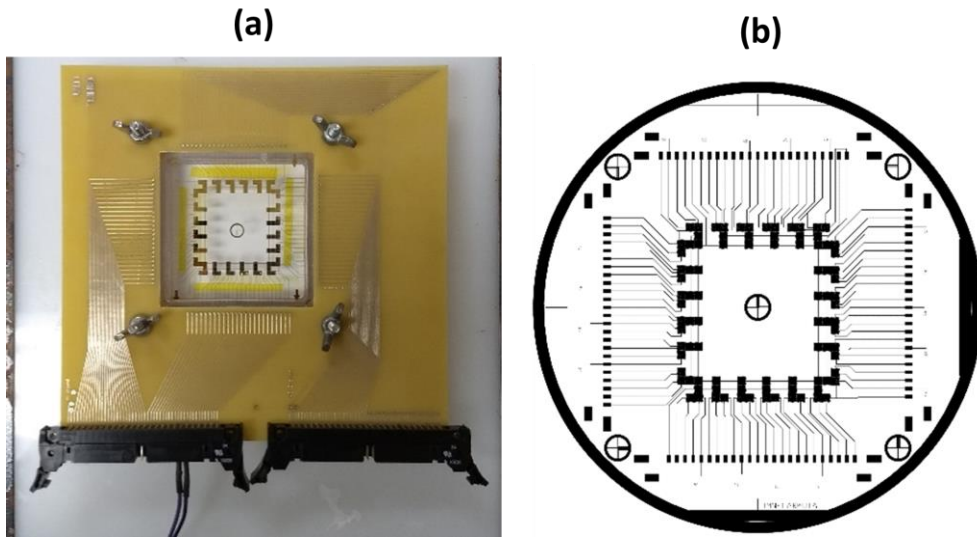


Figure 3-2 Off-chip sensing platform (a) Actual Setup (b) Mask for patterning Au on wafers

As shown in Figure 3-2, an array of sensors was used to perform calibration of calcium and sodium selective sensors in regard to their standard chloride solutions.

3.3 Results & Discussion

3.3.1 *calibration of sodium selective sensor*

Droplets ($3 \mu\text{l}$) of each molarity were dispensed over the fabricated sodium ion-selective electrode, and EMF was measured with a high input impedance ($\sim 10^{12} \Omega$) by HP 34401A Multimeter at room temperature (23°C). This experiment was repeated 3 times to ensure the reproducibility of data.

Activity coefficient of sodium ion in each sample has been calculated from the concentration of sodium ion, its ionic strength in the presence of chloride ion. Table 3-3

lists the data of experiments, and Figure 3-3 shows the time vs. EMF measurement of different molarity samples.

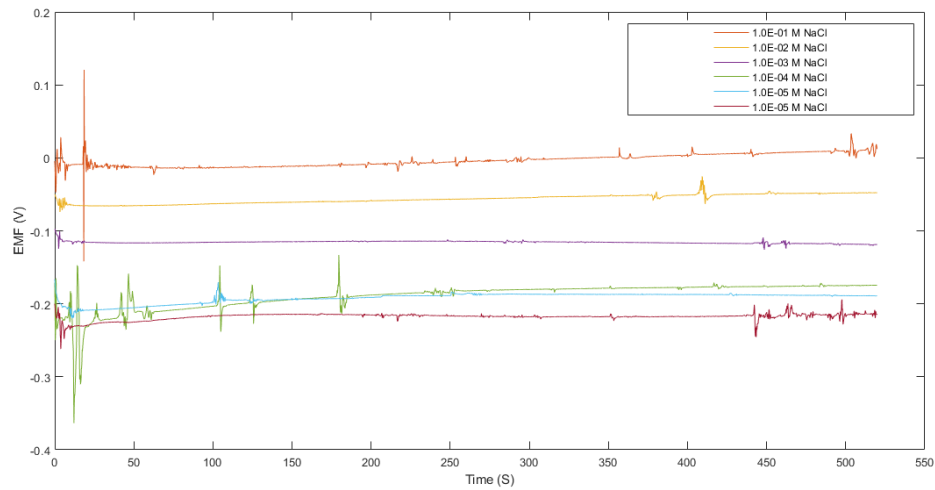


Figure 3-3 EMF measurement by the sodium selective sensor with respect to time

As seen in the figure 3-3, EMF output (within detection limit) from the sensor is well stabilized within 30 seconds. Therefore we chose $t=30$ for calibration of sodium selective sensor.

Table 3-3 EMF responses of different molarities of NaCl solutions in three experiments

@ $t=30$ s.

| Molarity (M) | Log(a(Na+)) | EMF 1 | EMF 2 | EMF 3 | Average ± STD |
|--------------|-------------|------------|----------|-----------|-------------------|
| 1.00E-06 | -5.97 | -0.225775 | -0.22732 | -0.20246 | -0.2185 ± 0.0113 |
| 1.00E-05 | -4.97 | -0.208039 | -0.20606 | -0.21436 | -0.212 ± 0.00354 |
| 1.00E-04 | -3.97 | -0.222182 | -0.21376 | -0.22444 | -0.2201 ± 0.00459 |
| 1.00E-03 | -2.98 | -0.116189 | -0.11513 | -0.11621 | -0.1158 ± 0.0005 |
| 1.00E-02 | -2.02 | -0.0657199 | -0.06357 | -0.06508 | -0.0647 ± 0.0009 |
| 1.00E-01 | -1.09 | -0.0134197 | -0.0132 | -0.013401 | -0.0133 ± 0.0009 |

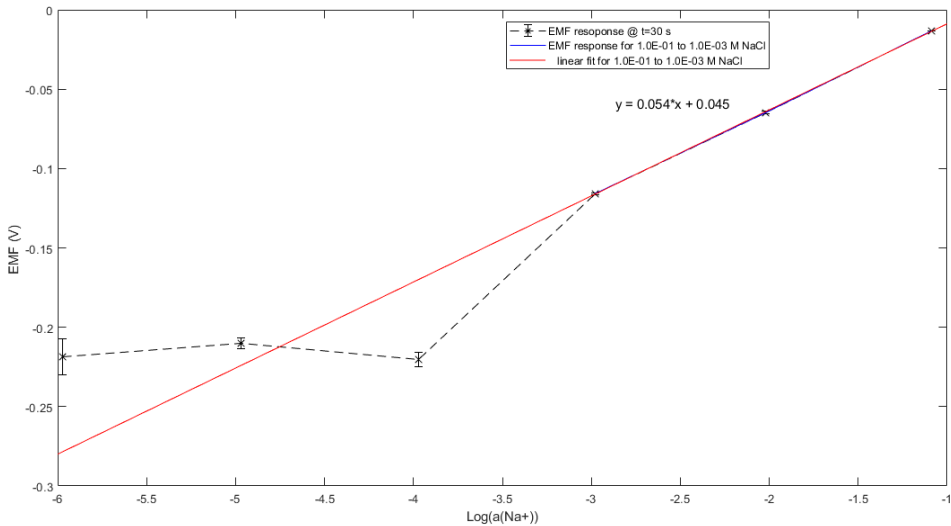


Figure 3-4 Calibration curve for average EMF (electromotive force) @ t=30 seconds

As mentioned in Section 3.2.1 the membrane composition was outsourced from Sigma Aldrich, and according to their reported data, this composition of sodium selective membrane is only linear in 10^{-1} to 10^{-3} M NaCl solutions, which is matched with the experimental value.

Although the detection limit will not cover from 10^{-3} to 10^{-6} M, this sensor can be used for measuring the sodium ion concentration in the human blood due to the compatibility of the range of sodium ion in human blood (Table 3-1) within its detection limit.

The Slope of experimental data is matched with the reported slope by Sigma Aldrich.

The selectivity coefficients $\text{Log}K_{\text{Na},M}^{\text{Pot}}$ as obtained by the separate solution method (0.1 M solutions of chlorides) reported by Sigma Aldrich are as follows:

$$\text{Log}K_{\text{Na},\text{Li}}^{\text{Pot}} = -0.4, \text{Log}K_{\text{Na},\text{K}}^{\text{Pot}} = -2.3, \text{Log}K_{\text{Na},\text{Ca}}^{\text{Pot}} = -0.2, \text{Log}K_{\text{K},\text{Mg}}^{\text{Pot}} = -2.4$$

Moreover, the slope of linear regression: 53.0 ± 2.5 mV (10^{-1} to 10^{-3} M NaCl)

3.3.2 calibration of calcium selective sensor

Droplets ($3\mu\text{l}$) of each molarity were dispensed over the fabricated calcium ion-selective electrode, and EMF was measured with a high input impedance ($\sim 10^{12} \Omega$) by HP 34401A Multimeter at room temperature (23°C). This experiment was repeated 3 times to ensure the reproducibility of Data, Activity coefficients of the calcium ion in each sample has been calculated from the oncentration of calcium ion, its ionic strength in presence of chloride ion. Table 3-4 lists the data of experiments and Figure 3-5 shows the time vs .EMF measurement of different molarity samples.

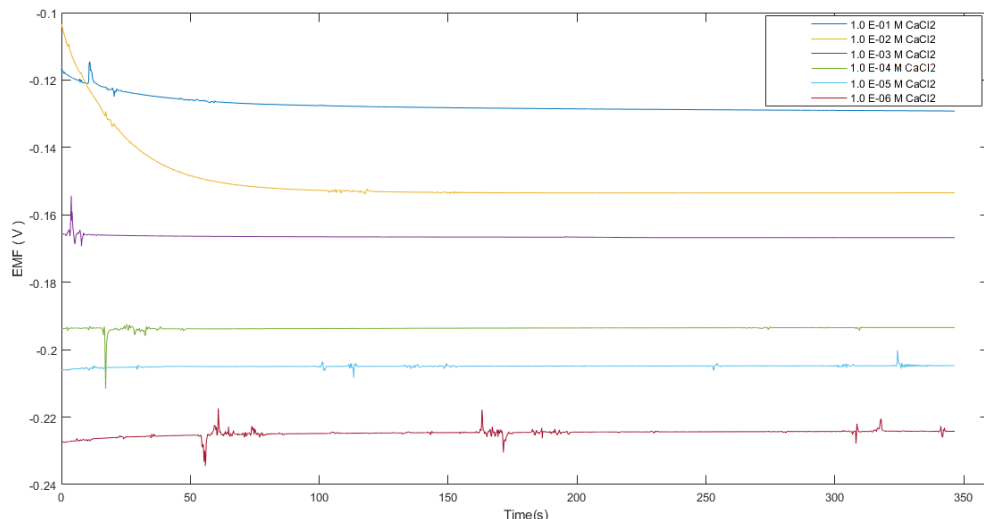


Figure 3-5 Electromotive force measurement by calcium selective sensor with respect to time

Table 3-4 Electromotive responses of different molarities of CaCl_2 solutions in three experiments @ $t=30\text{s}$.

| Molarity (M) | Log(a(Ca++)) | EMF 1 (V) | EMF 2 (V) | EMF 3 (V) | Average ± STD |
|--------------|--------------|------------|-----------|-----------|------------------|
| 1.00E-06 | -5.97 | -0.225775 | -0.22732 | -0.22246 | -0.2251 ± 0.0020 |
| 1.00E-05 | -4.97 | -0.205039 | -0.20606 | -0.20821 | -0.2071 ± 0.0013 |
| 1.00E-04 | -3.97 | -0.19354 | -0.19245 | -0.19306 | -0.193 ± 0.0004 |
| 1.00E-03 | -2.98 | -0.166189 | -0.16751 | -0.16723 | -0.1669 ± 0.0005 |
| 1.00E-02 | -2.02 | -0.1407199 | -0.141231 | -0.14236 | -0.1414 ± 0.0006 |
| 1.00E-01 | -1.09 | -0.1241978 | -0.12267 | -0.12101 | -0.1226 ± 0.0013 |

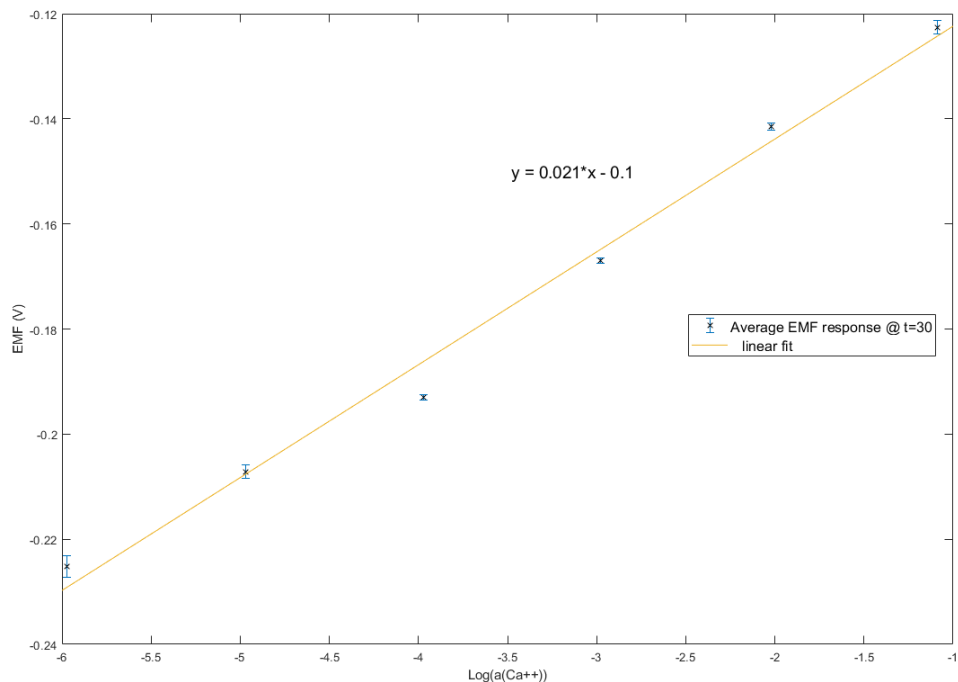


Figure 3-6 Calibration curve of Calcium ion selective sensor for average EMF (electromotive force) @ $t=30$ seconds

To validate the sensor, the slope Nernstian response of the fabricated sensor was compared with the theoretical value. As shown in Figure 3-6, EMF averaged data at $t = 30$ s were plotted to calibrate the sensor. The plot has a slope of 21 mV/log which is within the acceptable range (21 – 23 mV/log) for a successful calcium ion selective sensor according to the theory of potentiometric sensor.

The ionophore used in this cocktail is extremely lipophilic Ca^{2+} -selective ionophore for chemical sensors of long lifetime and the selectivity coefficients $\text{Log}K_{Na,M}^{\text{Pot}}$ reported by Sigma Aldrich are as follows:

$$\text{Log}K_{Ca,K}^{\text{Pot}} = -8, \text{Log}K_{Ca,Na}^{\text{Pot}} = -6, \text{Log}K_{Ca,Mg}^{\text{Pot}} = -4$$

It is important to mention that since we used the same membrane composition mentioned in chapter 2 for measuring potassium ion concentration, therefore, an off-chip calibration for potassium ion selective electrode was not discussed in this section.

3.3.3 Simultaneous measurement multiple ions via EWOD chip

In this experiment, a proof of concept demonstration of integration of electrolyte assay into EWOD was investigated. As shown in Figure 3-7, calcium, sodium and potassium selective sensor was fabricated on an EWOD chip without using the EWOD microfluidic functionality.

For this experiment, an emulated human blood plasma solution was made to experiment with EWOD chip. The concentrations of Ca^{2+} , Na^+ , and K^+ ions in the electrolyte were decided based on the range of concentration of these ions in the human blood (according to table 3-1). Therefore, a mixed solution with 1.4E-01 M Na^+ , 2.0E-03 M Ca^{2+} and 3.5E-03 M K^+ was prepared.

A droplet (7 μl) of the sample solution was dispensed over one of the EWOD chip reservoirs; then three smaller droplets were dispensed from the reservoir and brought

over the off-chip fabricated sensor via EWOD actuation. Then the EMF was measured simultaneously for each sensor.

it is important to mention that, the potentiometric selectivity coefficients are expressed according to the Nicolsky-Eisenman as

$$E = E_0 + \frac{RT}{Z_A F} \ln[a_A + \sum_B K_{A,B}^{Pot} (a_B)^{Z_A/Z_B}] \quad (18)$$

Where

E is the measured potential,

E_0 is a constant that includes the standard potential of the electrode, the reference electrode, and the junction potential,

Z_A and Z_B charge number of primary ion, A, and interfering ion, B,

a_A and a_B are the activities of primary ion, A, and interfering ion, B,

and $K_{A,B}^{Pot}$ is the potentiometric selectivity coefficient for primary ion A against the interfering ion B.

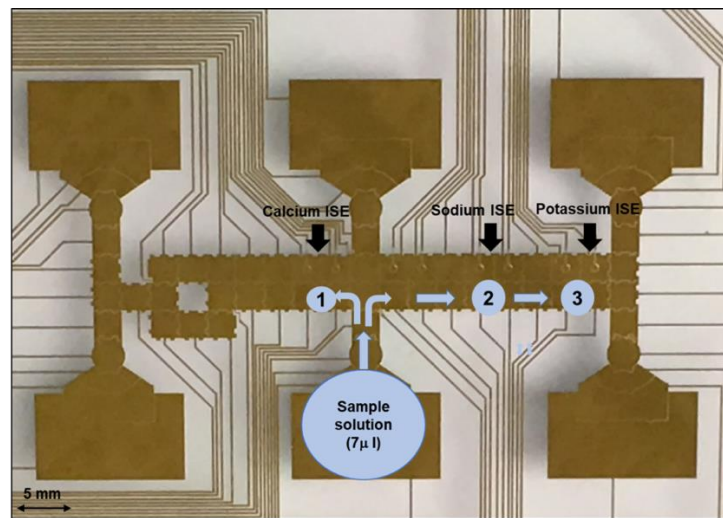


Figure 3-7 simultaneous measurement of Ca^{2+} , K^+ , Na^+

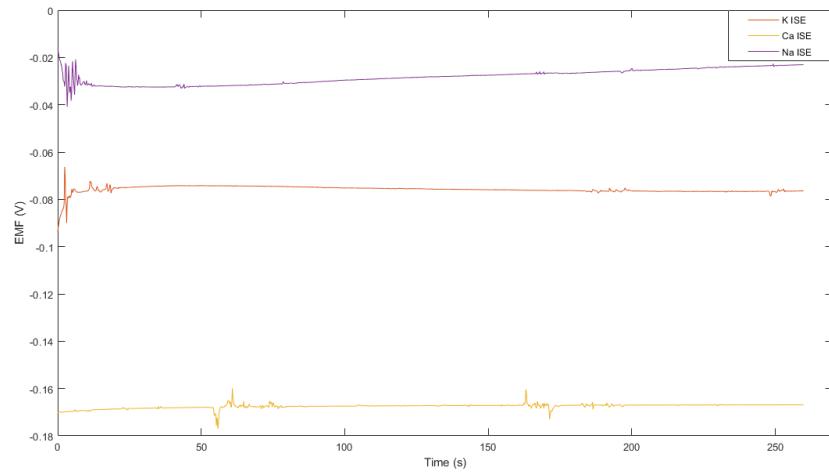


Figure 3-8 Electromotive force measurement by Ca^{2+} , K^+ , Na^+ selective sensor with respect to time.

With having the EMF measurement at the time $t=30$ second form the experiment (figure 3-8) along with having the calibration graphs from sections 2.3 (for potassium) and 3.3 (for calcium and sodium) and knowing the selectivity coefficient reported for each selective membrane, the ion activity of potassium, sodium, and calcium ion in the sample solution can be calculated.

$$K(A) = a_A + K_{A,B}^{Pot}(a_B)^{Z_A/Z_B} + K_{A,C}^{Pot}(a_c)^{Z_A/Z_C} \quad (19)$$

Where $K(A)$ is the value taken from the calibration curve based on the EMF response and A, B, C are the ions.

Three equations can be written according to three responses. Solving for these three unknowns, three-equations through Fsolve in Matlab resulted in following activities:

$$a_{Na+} = 1.36 \times 10^{-1}, a_{Ca++} = 2.05 \times 10^{-3}, a_{K+} = 3.51 \times 10^{-3}$$

The error percentages for K^+ , Na^+ and Ca^{2+} are 0.28%, 2.85% and 2.5% respectively.

3.3 Conclusion & outlook

In the proposed lab on a chip, the sample volume required for the measurements of the concentration of the Ca^{2+} , K^+ and Na^+ is in the order of 10 microliters compare to conventional methods which is in order of tens of milliliter, resulting in a massive reduction in reagent consumption, which eventually results in a more cost-effective screening. Additionally, the capability of the proposed microfluidic system in the handling of nanoliter-scale reduced the necessary blood sample amount for each test and resulted in a transition from vein acquisition to fingertip acquisition.

Capability of simultaneous measurement and automation in proposed LOC can minimize the common human error involve with healthcare diagnostic processes and drastically reduce time required for analysis.

The availability of such a device with the ability of rapid fingertip acquisition and analysis will create possibilities like emergency room BMP screening and eliminate the blood vein acquisition problems in elderly patients.

Additionally, the affordability of the test conducted by the proposed devices can have a significant impact on dietary adjustments since the BMP monitoring can happen more frequently and the result can be recorded for comprehensive analysis throughout the patient's lifetime.

Chapter 4

Towards liquid-liquid electrochemical bio-sensor enabled by an EWOD Platform

4.1 Literature summary & motivation

liquid-liquid extraction (LLE) is an important pretreatment technique used in many chemical/biomedical processes. Aqueous two-phase system (ATPS) is emerged as powerful tools in LLE for efficient extraction and purification of enzymes due to their versatility, lower cost.

For example, The recoveries of high-value biomolecules were achieved from various plants using different applications of ATPS such as extraction of papain from Papaya fruit and α - and β -amylases from Zea mays malt [37]. While ATPS has been very popular in large-scale downstream separation and purification processes, its application to microscale process is relatively unexplored. Pavithra et al., successfully conducted an microscale liquid-liquid extraction with the preparation of ATPS droplets on EWOD DMF chips and found that the quality of ATPS formed on-chip is very close to that of ATPS formed at the macroscale [38].

Most LLE studies used conventional optical measurement systems in their analysis to confirm their quality of extraction and purification. Therefore, the need for integration of a cheap analysis system to LLE systems still exists.

Introducing an impedimetric electrochemical measurement into LLE platforms can result in portable and efficient extraction devices. On the other hand, liquid-liquid extraction as a mechanism can be integrated with impedimetric electrochemical measurement for an immobilization-free measurement.

In liquid-liquid extraction systems for a given compound, its solubility between two solvents is given by the quantitative measure called distribution coefficient (i.e., partitioning coefficient). While partition coefficient can be modified by doping the structure of one of the

solvents (i.e., extractant), choosing the extractant itself is crucial. Room temperature ionic liquids (RTILs) have been used as novel solvents to replace the traditional volatile organic solvents in the fields of organic synthesis, solvent extraction, and electrochemistry. The hydrophobic character and water immiscibility of certain ionic liquids allow their use in solvent extraction of hydrophobic compounds. Wei et al. used a typical ionic liquid, 1-butyl-3-methylimidazolium hexafluorophosphate for extracting metal ions from aqueous solution by employing Dithizone as the metal chelator [39].

Another advantage of ionic liquids is their synthesizability and its ability to be designed with specific thermophysical and electrophysical properties for a specific application. Yang also studied the selectivity of different ionic liquids towards Tocopherol Homologues by using liquid-liquid extraction and found out that the selectivity in the extraction process is significantly affected by the anions of the IL [16].

In this study, we are proposing a liquid-liquid electrochemical sensor integrated into EWOD electrodes, in the proposed sensor an ionic liquid mixed with potassium ionophore was used as an extractant and different molarities of KCl solutions were used as sample solutions. EIS was used for impedance measurement of modified ionic liquid before and after the sample solution interaction. A normalized number which is the high frequency impedance difference of the modified ionic liquid (extractant) before and after of sample interaction was used for calibrating the sensor.

4.2 Sensing Scheme

Test scheme is as follows, at first, one droplet (3 μ l) of ionic liquid containing potassium ionophores dispensed over an interdigitated electrode integrated into EWOD

electrode. With acquiring a first electro impedance spectra (EIS) and fitting it to our equivalent circuit model, the initial values of electrical parameters of our modified liquid was recorded. Then the sample droplet which is our KCl solution containing potassium ion was dispensed over next to modified ionic liquid and creates a liquid-liquid junction. Due to the functionality of ionophore, the ions will attach or transfer to ionic liquid medium (i.e., modified droplet). Finally, with removing the sample liquid from the interface, we perform another EIS to find the secondary value of components of the equivalent circuit of modified liquid. The difference between the initial and secondary value of electrical elements correlated to the concentration of targeted biomolecule in the sample solution.

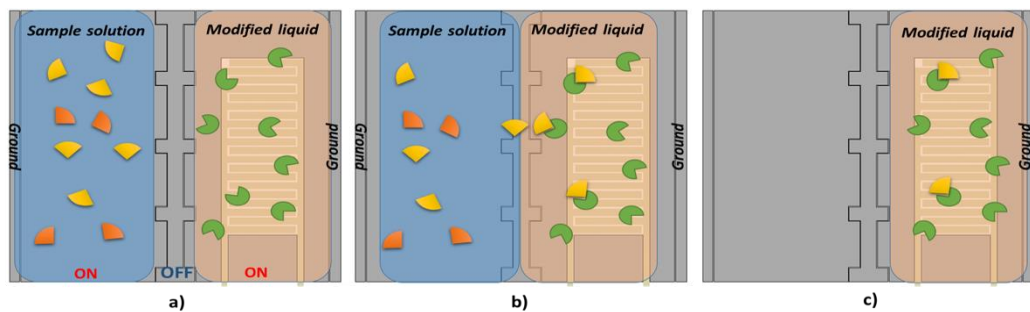


Figure 4-1 Liquid-liquid Testing scheme.

a) The modified ionic liquid (liquid containing ionophore) dispensed over the sensing electrode, and an EIS acquired for determination of initial values. b) The sample solution dispensed over the next electrode, then with activation the central electrode an interface will form between 'modified liquid' and "sample liquid. c) By removing the sample liquid from the interface, another EIS acquired to find the secondary values

4.3 Material & Methods

4.3.1 Material

Gold (Au, 1000 Å)/ Chromium (Cr, 100 Å) coated glass wafer was used to fabricate the integrated device. Metal layers (Au/Cr) were used for EWOD electrodes as well as interdigitated electrodes (IDE). S1813 (MICROPOSIT) was used as the photoresist for patterning and mask layer in different stages of chip fabrication. SU-8 2005 (Micro-Chem) was used as the dielectric layer. Teflon AF1600S (Du Pont) powder dissolved in Fluorinert FC-40(Sigma-Aldrich) solution was used as the hydrophobic layer on top of the dielectric layer.

1-Ethyl-3-methylimidazolium bis(trifluoromethylsulfonyl)imide a hydrophobic ionic liquid has been purchased from Iolitec. This Ionic liquid has high electrochemical window makes them compatible with non-faradaic electrochemical sensors. Table 4-1 represent physicochemical properties of the ionic liquid.

Table 4-1 physicochemical properties of 1-Ethyl-3-methylimidazolium
bis(trifluoromethylsulfonyl)imide

| | |
|---------------------------|--|
| Melting point | -16 °C |
| Density | 1.52 g/cm ³ |
| Viscosity | 35.55 cP @ 25°C |
| Decomposition Temperature | 455°C |
| Electrochemical window | 4.7 V @ RT (1mA/cm ²) |
| Conductivity | 9 mS/cm @ RT |
| Miscible in | Acetonitrile, acetone, dichloromethane, DMSO |
| Immiscible in | Water, hexane, diethyl ether |

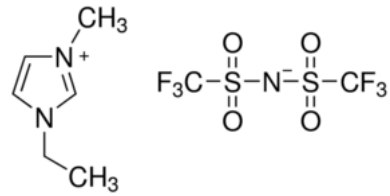


Figure 4-2 Chemical formula of 1-Ethyl-3-methylimidazolium bis(trifluoromethylsulfonyl)imide.

Regarding choosing the selectivity of our ionic liquid, Potassium ionophore dissolved in tetrahydrofuran (THF) then mixed with the IL. It is worth to mention that the usage of THF as an organic solvent is a standard method for fabrication of ion-selective membranes (ISM).

Later the mixture was placed in the oven for evaporating the THF. Dehydration process of the ionic liquid is standard due to their high absorption of water. Bath sonication also has been used for enhancing the mixing of ionophore and ionic liquids during the mixing process.

It is important to mention that; there have been studies in regard to the usage of ionic liquid in the structure of ion-selective membrane in the construction of Cu(II) ion-selective electrode with solid contact [31]. However, in these types of sensors, the ionic liquid usually replaces the plasticizer in the structure of the ISMs, and since the gel phase Membrane layer is desired, the PVC has been used for forming the structure.

However, In this study, we chose to use 98% ionic liquid and 2% potassium ionophore as the liquid phase to perform the liquid-liquid extraction.

The choice of weight percentage for potassium ionophore in the extractant liquid was based on their standard weight percentage in potassium ISMs,

Ionophores are organic molecules that are insoluble in aqueous solutions which make them perfect match as the recognition element for LLE based electrochemical sensing.

In this study, an interdigitated electrode arrays (IDEA) to measure impedance changes in non-Faradaic measurements. For acquiring Electro impedance spectroscopy (EIS), The Reference 300 from Gamry instrument has been used.

The EIS data was fit using EChem AnalystTM (Gamry Instruments, Warminster, PA, USA). For acquiring the calibration curve, different molarities of KCl solution ($1\mu\text{M}$ - 1M) were prepared by serial dilution of stock solution (1 M KCl). The stock KCl solution was prepared by dissolving potassium chloride powder (Sigma-Aldrich) in deionized water.

4.3.2 Sensor Design & equivalent circuit model considerations

Our goal is to design and test sensor which has the compatibility with EWOD DMFs. Integrating electrochemical biosensors into EWOD has two main challenges: (1) complete removal of the droplet containing the analyses from the sensing surface; and (2) biochemical regeneration of the biorecognition element immobilized on sensor electrode after each round of measurement [29].

In our proposed sensor, we are eliminating the second problem by using liquid-liquid extraction method where the biorecognition element entrapped in a desired ionic liquid. However, for enhancing the droplet removal, Samiei conducted experiments studied the effect of the ratio between the actuating electrode and sensor electrode (i.e., The hydrophilic-to-hydrophobic ratio) on movability of the droplets.

With knowing that the signal derived from the sensor electrode is dependent on the sensor area, we chose a 33% as our ratio to achieve movability in proposed microfluidic devices while having maximum area possible.

Although in this study we did not perform the liquid-liquid sensing on EWOD DMF, we did use the electrowetting for controlling interface between the Ionic liquid and sample solutions. Figure 4-2 shows the IDE (i.e., Interdigitated Electrodes) used in our experiments.

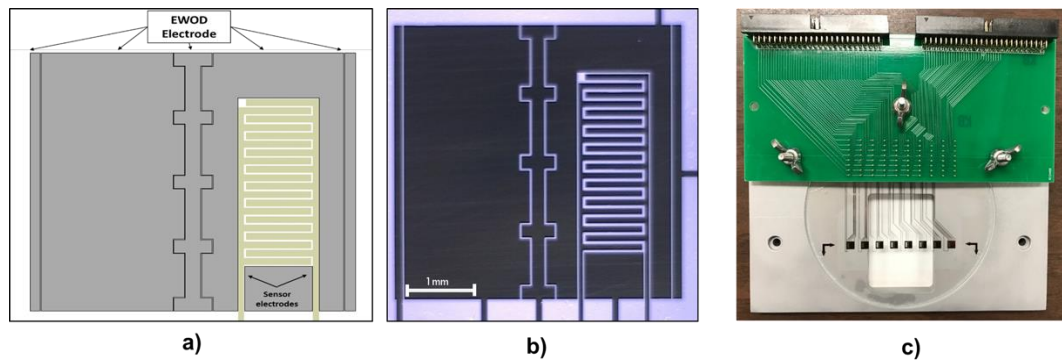


Figure 4-3 Interdigitated electrode integrated on EWOD electrode.

a) Schematic of sensor b) Actual photo of IDE c) Sensing platform

In recent studies, it has been demonstrated that the change in the contact angle of the droplet can change the RC (resistor-capacitor) behavior of the ionic liquid. Nanayakkara et al. create a tunable RC filter using ionic liquids and electrowetting on the dielectric[33]. Therefore, in our sensor, we measure the impedance of electrochemical cell (i.e., modified ionic liquid) and since this impedance can be affected by the contact angle of the droplet on IDE, we used hydrophilic opening and EWOD electrodes to control the contact angle and time of the interface formation.

Development of an equivalent circuit for an electrochemical cell is essential and necessary for collecting quantitative information on parameter variations. However, these models can vary in different systems. An Ideal circuit can deviate from values measured in the experiment which usually can be corrected by considering phenomena like Ionic chemical/physical adsorption, diffusional impedance, and Incomplete polarization. Yang et al. develop a model for interdigitated impedance immune sensor for detecting E coli [40]. Wang et al. also develop a circuit model for quantification of their EIS data for a capacitive DNA biosensor in different stages of the sensor[41].

In our experiment two equivalent circuits have been developed for the proposed IDE sensor since during the LLE potassium ions are getting transferred which changes the electrical behavior of the modified ionic liquid. The figure 4-4 shows the equivalent circuit model for Initial EIS.

As shown in the figure 4-4, the electrochemical cell of IDEs are presented by an electric double layer capacitance(CPE_{dl}), Resistance at double later interface (R_{int}), bulk capacitance(CPE_{bulk}), bulk resistance (R_{bulk}) and the solution resistance (R_s).

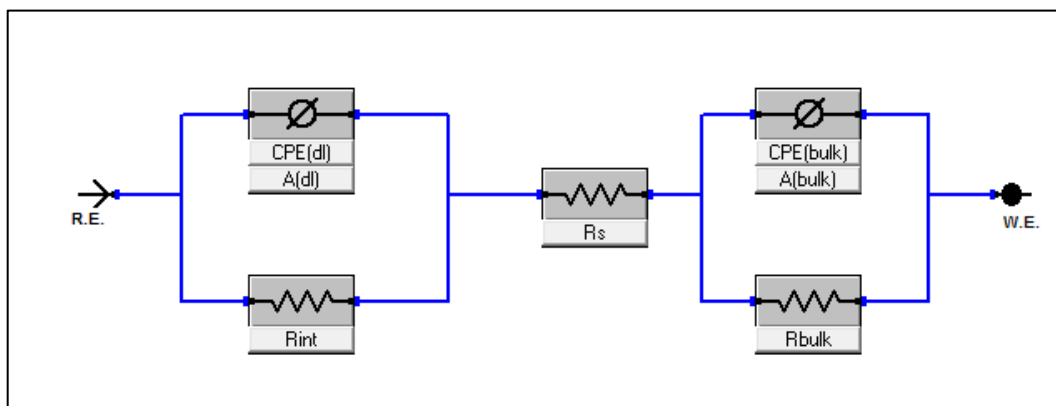


Figure 4-4 Equivalent circuit for Initial EIS Data

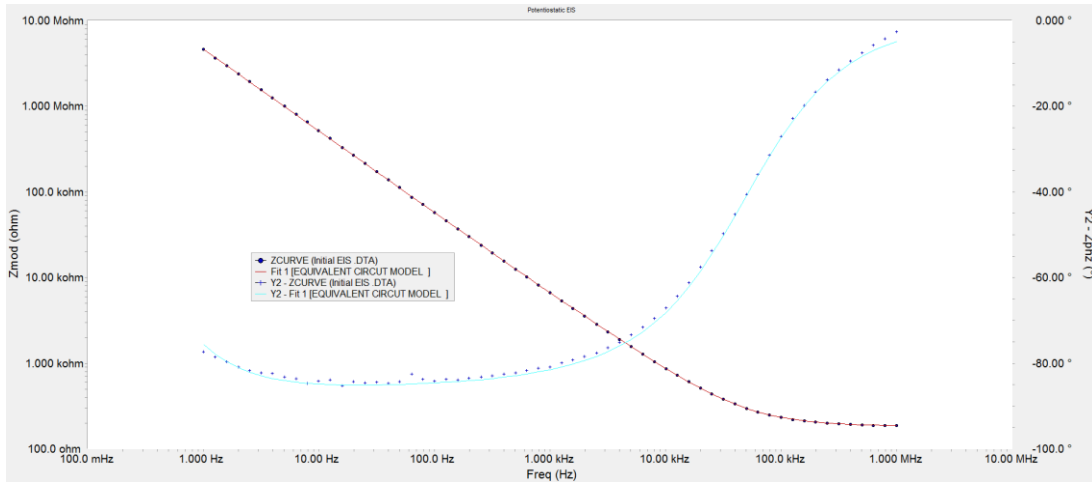


Figure 4-5 Curve fitting of initial experimental data with the model (The bode plot)

The curve fitting of the EIS response of the electrochemical cell to the response of equivalent circuit model was performed via Reference 300 Gamry data analyzer software which has an agreement factor of 2×10^{-6} .

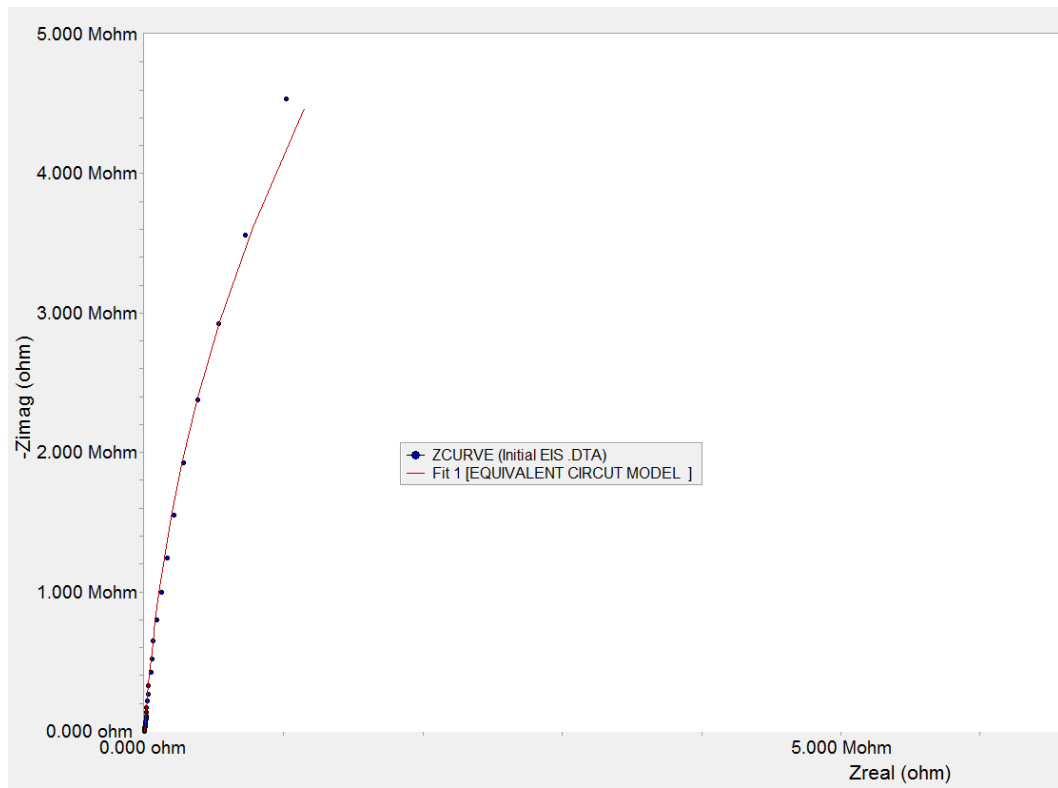


Figure 4-6 Curve fitting of initial Experimental Data with model (The Nyquist plot)

Figure 4-5 and 4-6 show the good agreement between the response of modeled equivalent circuit (figure 4-4) and experimental data in the Bode and Nyquist plot for the initial response of the modified ionic liquid.

Transferring potassium ions can introduce the diffusion resistance after EDL in bulk layer which can be represented by a Warburg element in the model and the entrapment of ions within the electrode array can be presented by a capacitor as shown in figure 4-7.

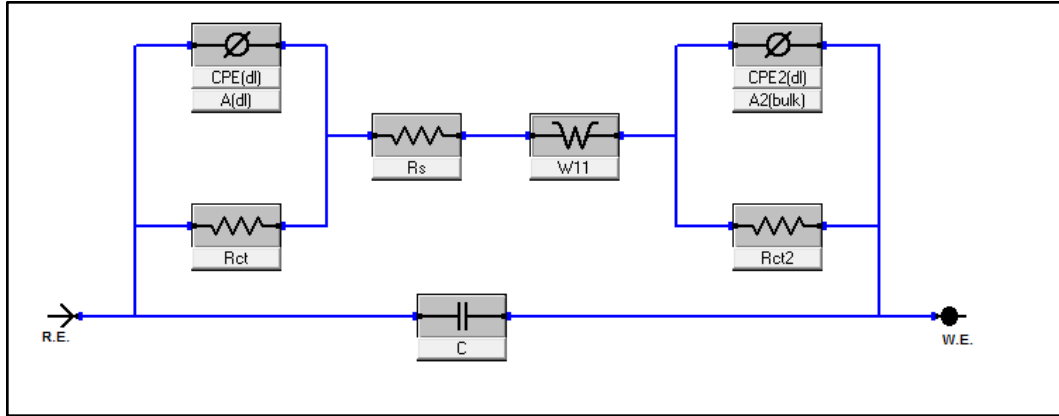


Figure 4-7 Equivalent circuit for secondary EIS Data

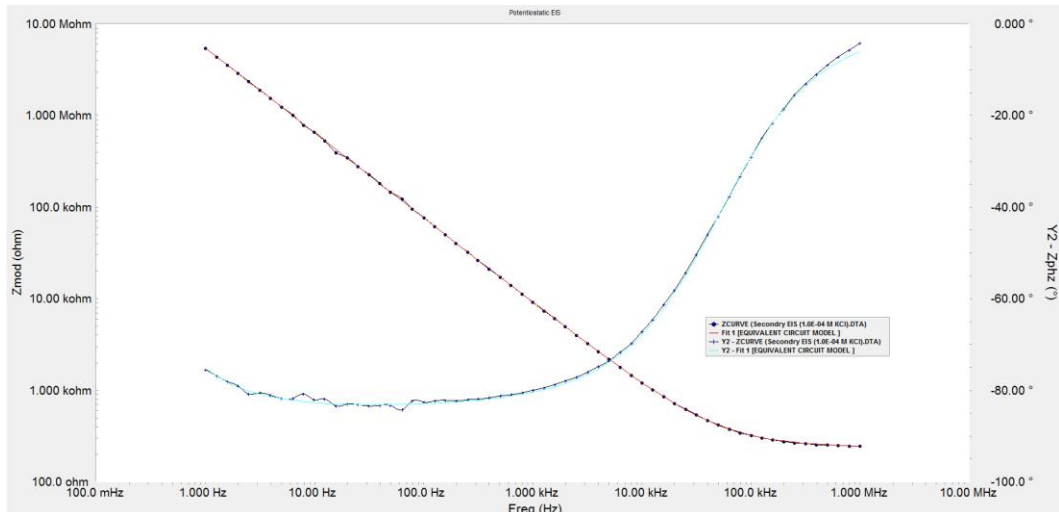


Figure 4-8 Curve fitting of secondary experimental data with the equivalent circuit model
(The bode plot)

Figure 4-8 shows the good agreement between the response of modeled equivalent circuit (figure 4-7) and experimental data with the Bode for the secondary response of the modified ionic liquid.

4.3 Initial results and discussion

In impedance spectroscopy of an electrochemical cell, the impedance of high frequency is representing the resistance of the liquid since the impedance of capacitance approaching zero in high frequencies. Therefore, we used impedances differences obtained at high frequencies to avoid the complexity of capacitance behavior in lower frequencies however for complete analysis,

Although the equivalent circuit model mentioned in the last section was developed to investigate the EIS data of electrochemical cell, but for using of the calculated values (through fitting the response of the equivalent model and EIS data) , a more comprehensive analysis is required for changes of modified ionic liquid before and after the sample interaction.therefore in this study the impedances in high frequency has been used for calculating calibration graphs.

For determination of the selectivity of 1-Ethyl-3-methylimidazolium bis(trifluoromethylsulfonyl)imide without adding the potassium ionophores towards potassium ion, six tests with different KCl molarity (i.e., sample solution) and Pure IL (i.e., selective medium) has been conducted. The figure below shows that the ionic liquid itself does not have the selectivity towards potassium ions.

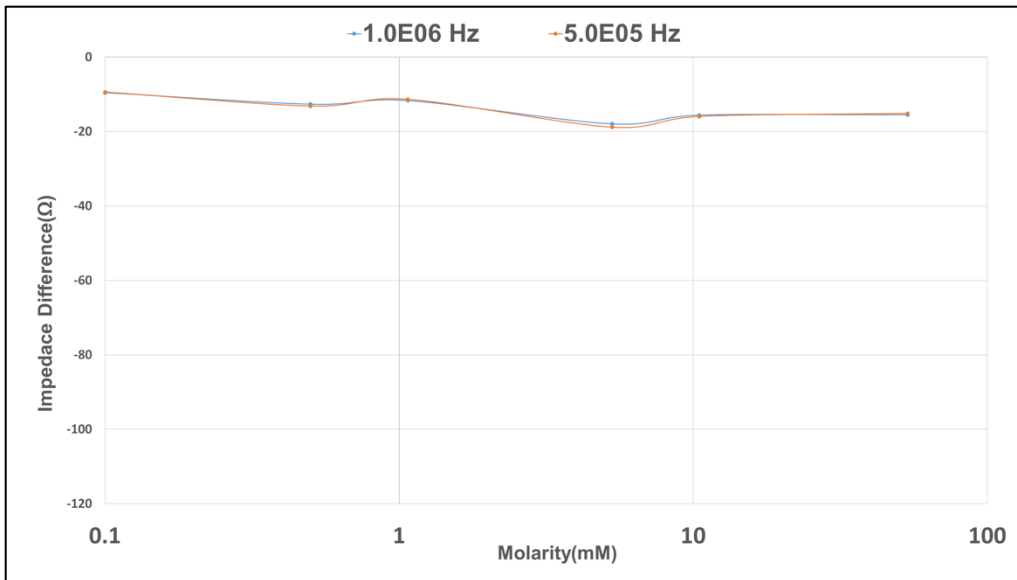


Figure 4-9 Pure Ionic Liquid as a selective medium in LLE

To confirm the repeatability of Modified ionic liquid (i.e., Ionic liquid mixed with ionophore), EIS of seven different sample has been acquired and compared.

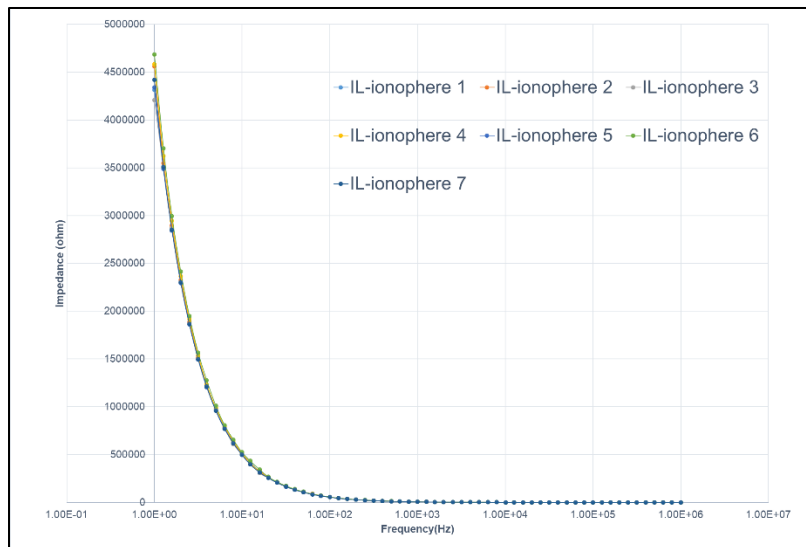


Figure 4-10 Electro impedance spectroscopy of initial values

Table 4-2 Standard deviations of initial impedance values of modified ionic liquid

| Frequency (HZ) | Standard deviation (Ω) |
|----------------|---------------------------------|
| 1.0E06 | 0.435622 |
| 5.0E05 | 0.791459 |
| 1.0E05 | 4.824511 |
| 5.0E04 | 10.83199 |

As shown in Figure 4-10 and Table 1-2 their standard deviation is below 0.5 % in high frequency showing the consistency in our initial EIS values for each test.

Finally, after dispensing the KCl solutions and acquiring secondary impedance values, we found that impedance difference is lower for the sample with a higher concentration of Potassium. This can be explained by the intrinsic behavior of Ionophores which act as ion carrier in an organic medium and the fact that they form complexes in the presence of targeted ions when in contact with sample solutions.

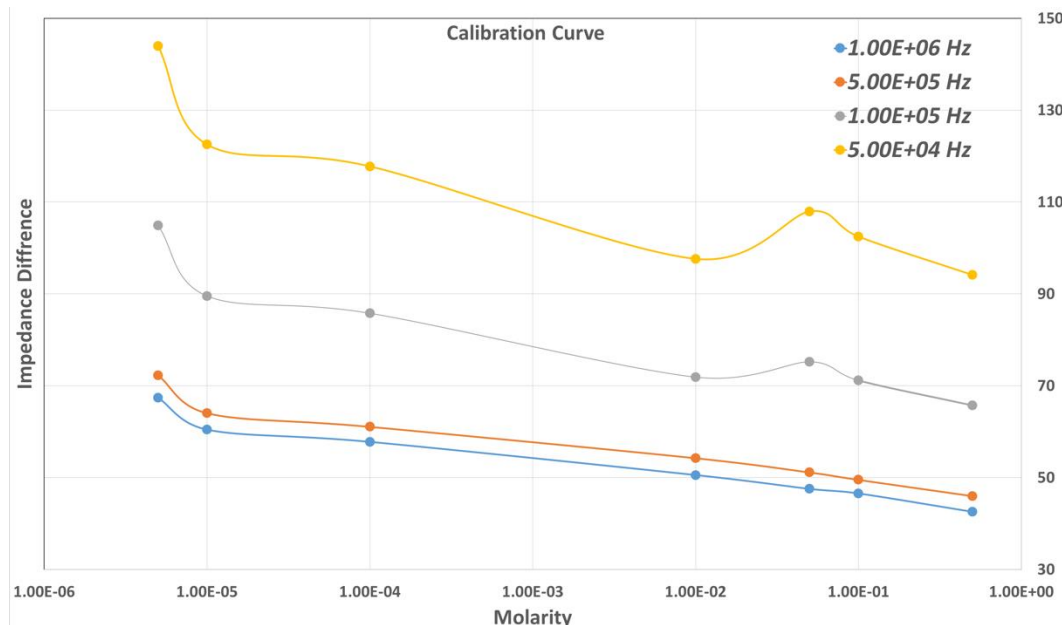


Figure 4-11 Impedance difference Vs. KCl sample concentration

4.4.Conclusion & outlook

This work is a demonstration of proof of concept liquid-liquid bioelectrochemical sensor which is perfectly compatible with digital microfluid devices.

For the first time instead of a hydrogel or polymeric membrane (which is commonly used), a modified ionic liquid as a selective medium for the impedimetric measurement.

In this proposed electrochemical sensor, unlike any other sensor, the selective element (enzyme, antibody, ionophores) is not immobilized on the surface of the electrode, whereas the selective element is mixed with the ionic liquid which results in less inactivation due to a controlled environment. Although More studies needed for determining the static and dynamic characteristics of proposed sensor This characteristic itself make the fabrication of the bio-sensors much more comfortable and more variable. It is worthy to say that biosensors are widely used in medical diagnostics, biological research, environmental protection, and food analysis where one of the significant hurdles is immobilizing the selective element. The introduced sensor is the perfect match for Digital Microfluidics (i.e., EWOD) where liquids (~650 nL) are manipulated as droplets by applying electrical potential on series of electrodes with the dielectric layer on top. This integration of sensor and EWOD will pave the path to low cost and compatible home-use sensors where ease of use, automation and minimal consumption of reagents is crucial.

Chapter 5

Conclusion

This work outlines a study of the integration of electrochemical sensors into digital microfluidics (DMF) electrowetting on dielectric (EWOD) by designing and testing two proof-of-concept systems for introducing reconfigurability on lab on a chip (LOC) devices and an assay for simultaneous measurement via one drop.

1. Presented a demonstration of a reconfigurable potentiometric ion-selective electrode (ISE) array enabled by an electrowetting-on-dielectric (EWOD) microfluidic platform.
2. On-chip fabrication of Ag/AgCl via EWOD microfluidic devices was investigated
3. Simultaneous measurement of K⁺, Na⁺ and Ca²⁺ ion concentration in a droplet of human blood plasma emulated solution.
4. A proof of concept of a liquid-liquid electrochemical sensor was investigated for elimination the immobilization process on sensor electrodes

References

- [1] H. Moon, S. K. Cho, R. L. Garrell, and C. J. Kim, "Low voltage electrowetting-on-dielectric," *J. Appl. Phys.*, vol. 92, no. 7, pp. 4080–4087, 2002.
- [2] R. Digilov, "Charge-induced modification of contact angle: The secondary electrocapillary effect," *Langmuir*, vol. 16, no. 16, pp. 6719–6723, 2000.
- [3] S. K. Cho, H. Moon, and C. J. Kim, "Creating, transporting, cutting, and merging liquid droplets by electrowetting-based actuation for digital microfluidic circuits," *J. Microelectromechanical Syst.*, vol. 12, no. 1, pp. 70–80, 2003.
- [4] J. Lee, H. Moon, J. Fowler, T. Schoellhammer, and C. J. Kim, "Electrowetting and electrowetting-on-dielectric for microscale liquid handling," *Sensors Actuators, A Phys.*, vol. 95, no. 2–3, pp. 259–268, 2002.
- [5] W. C. Nelson and C. C. J. Kim, "Journal of Adhesion Science and Droplet Actuation by (EWOD): A Review," *J. Adhes. Sci. Technol.*, vol. 26, no. August 2012, pp. 1747–1771, 2012.
- [6] D. Grieshaber, R. MacKenzie, J. Vörös, and E. Reimhult, "Electrochemical Biosensors - Sensor Principles and Architectures," *Sensors*, vol. 8, no. 3, pp. 1400–1458, 2008.
- [7] D. R. Thévenot, K. Toth, R. A. Durst, and G. S. Wilson, "Electrochemical biosensors: Recommended definitions and classification," *Biosens. Bioelectron.*, vol. 16, no. 1–2, pp. 121–131, 2001.
- [8] A. Sassolas, L. J. Blum, and B. D. Leca-Bouvier, "Immobilization strategies to develop enzymatic biosensors," *Biotechnol. Adv.*, vol. 30, no. 3, pp. 489–511, 2012.
- [9] J. Hüller, M. T. Pham, and S. Howitz, "Thin layer copper ISE for fluidic microsystem," *Sensors Actuators B Chem.*, vol. 91, no. 1–3, pp. 17–20, Jun.

2003.

- [10] B. Peng, J. Zhu, X. Liu, and Y. Qin, "Potentiometric response of ion-selective membranes with ionic liquids as ion-exchanger and plasticizer," *Sensors Actuators, B Chem.*, vol. 133, no. 1, pp. 308–314, 2008.
- [11] R. P. Buck and E. R. N. Lindneri, "COMMISSION ON ELECTROANALYTICAL CHEMISTRY * RECOMENDATIONS FOR NOMENCLATURE OF ION-SELECTIVE ELECTRODES ion-selective electrodes (IUPAC," *Pure Appl. Chem.*, vol. 66, no. 12, pp. 2527–2536, 1994.
- [12] T. Zwickl, T. Sokalski, and E. Pretsch, "Steady-state model calculations predicting the influence of key parameters on the lower detection limit and ruggedness of solvent polymeric membrane ion-selective electrodes," *Electroanalysis*, vol. 11, pp. 673–680, 1999.
- [13] C. I. Values, P. Electrochemistry, C. Elements, C. Equivalent, and C. Models, "Basics of Electrochemical Impedance Spectroscopy," no. 1.
- [14] J. Lenik, C. Wardak, and M. Grabarczyk, "Application of ionic liquid to the construction of Cu(II) ionselective electrode with solid contact," *Procedia Eng.*, vol. 47, no. li, pp. 152–155, 2012.
- [15] R. Patel, M. Kumari, and A. B. Khan, "Recent advances in the applications of ionic liquids in protein stability and activity: A review," *Appl. Biochem. Biotechnol.*, vol. 172, no. 8, pp. 3701–3720, 2014.
- [16] Z. He and P. Alexandridis, "Nanoparticles in ionic liquids: interactions and organization.,," *Phys. Chem. Chem. Phys.*, vol. 17, no. 28, pp. 18238–61, 2015.
- [17] a. a. H. Padua, M. F. C. Gomes, and J. N. C. Lopes, "Molecular Solutes in Ionic Liquid Structural Perspective," *Acc. Chem. Res.*, vol. 40, no. 11, pp. 1087–1096, 2007.

- [18] H. Tokuda, K. Ishii, M. A. B. H. Susan, S. Tsuzuki, K. Hayamizu, and M. Watanabe, "Physicochemical properties and structures of room-temperature ionic liquids. 3. Variation of cationic structures," *J. Phys. Chem. B*, vol. 110, no. 6, pp. 2833–2839, 2006.
- [19] H. F. D. Almeida, A. R. R. Teles, J. A. Lopes-Da-Silva, M. G. Freire, and J. A. P. Coutinho, "Influence of the anion on the surface tension of 1-ethyl-3-methylimidazolium-based ionic liquids," *J. Chem. Thermodyn.*, vol. 54, pp. 49–54, 2012.
- [20] D. R. MacFarlane, N. Tachikawa, M. Forsyth, J. M. Pringle, P. C. Howlett, G. D. Elliott, J. H. Davis, M. Watanabe, P. Simon, and C. A. Angell, "Energy applications of ionic liquids," *Energy Environ. Sci.*, vol. 7, no. 1, pp. 232–250, 2014.
- [21] T. A. Cohn and M. J. Sernyak, "Metabolic Monitoring for Patients Treated With Antipsychotic Medications," *Can J Psychiatry*, vol. 51, no. 8, pp. 492–501, 2006.
- [22] M. J. Jebrail, M. S. Bartsch, and K. D. Patel, "Digital microfluidics: a versatile tool for applications in chemistry, biology and medicine," *Lab Chip*, vol. 12, no. 14, pp. 2452–2463, 2012.
- [23] K. Zhang, G. Tao, X. Zeng, W. Sheng, and J. Zhou, "Compact and portable chemiluminescence detector for glucose," *Proc. Int. Conf. ASIC*, 2013.
- [24] H. Arida, Q. Mohsen, and M. Schöning, "Microfabrication, characterization and analytical application of a new thin-film silver microsensor," *Electrochim. Acta*, vol. 54, no. 13, pp. 3543–3547, May 2009.
- [25] M. Odijk, E. J. Van Der Wouden, W. Olthuis, M. D. Ferrari, E. A. Tolner, A. M. J. M. Van Den Maagdenberg, and A. Van Den Berg, "Microfabricated solid-state ion-selective electrode probe for measuring potassium in the living rodent brain: Compatibility with DC-EEG recordings to study spreading depression," *Sensors*

Actuators, B Chem., vol. 207, no. PB, pp. 945–953, 2015.

- [26] E. Samiei, M. Tabrizian, and M. Hoorfar, “A review of digital microfluidics as portable platforms for lab-on a-chip applications,” *Lab Chip*, vol. 16, no. 13, pp. 2376–2396, 2016.
- [27] B. Kintses, L. D. van Vliet, S. R. A. Devenish, and F. Hollfelder, “Microfluidic droplets: New integrated workflows for biological experiments,” *Curr. Opin. Chem. Biol.*, vol. 14, no. 5, pp. 548–555, 2010.
- [28] Y. Yu, J. Chen, and J. Zhou, “Parallel-plate lab-on-a-chip based on digital microfluidics for on-chip electrochemical analysis,” *J. Micromechanics Microengineering*, vol. 24, no. 1, p. 15020, Jan. 2014.
- [29] E. Samiei, G. S. Luka, H. Najjaran, and M. Hoorfar, “Integration of biosensors into digital microfluidics: Impact of hydrophilic surface of biosensors on droplet manipulation,” *Biosens. Bioelectron.*, vol. 81, pp. 480–486, 2016.
- [30] A. Bratov, N. Abramova, and A. Ipatov, “Recent trends in potentiometric sensor arrays-A review,” *Anal. Chim. Acta*, vol. 678, no. 2, pp. 149–159, 2010.
- [31] B. J. Polk, A. Stelzenmuller, G. Mijares, W. MacCrehan, and M. Gaitan, “Ag/AgCl microelectrodes with improved stability for microfluidics,” *Sensors Actuators B Chem.*, vol. 114, no. 1, pp. 239–247, Mar. 2006.
- [32] H. Suzuki, T. Hirakawa, S. Sasaki, and I. Karube, “Micromachined liquid-junction Ag/AgCl reference electrode,” *Sensors Actuators B Chem.*, vol. 46, no. 2, pp. 146–154, Feb. 1998.
- [33] C. H. Chen, S. L. Tsai, M. K. Chen, and L. S. Jang, “Effects of gap height, applied frequency, and fluid conductivity on minimum actuation voltage of electrowetting-on-dielectric and liquid dielectrophoresis,” *Sensors Actuators, B Chem.*, vol. 159, no. 1, pp. 321–327, 2011.

- [34] H. F. Osswald, R. Asper, W. Dimai, and W. Simon, “On-line continuous potentiometric measurement of potassium concentration in whole blood during open-heart surgery,” *Clin. Chem.*, vol. 25, no. 1, pp. 39–43, 1979.
- [35] S. Graham, “For Organic Electronics,” vol. 5, pp. 289–293, 1970.
- [36] P. K. Whelton, L. J. Appel, R. L. Sacco, C. A. M. Anderson, E. M. Antman, N. Campbell, S. B. Dunbar, E. D. Frohlich, J. E. Hall, M. Jessup, D. R. Labarthe, G. A. Macgregor, F. M. Sacks, J. Stamler, D. K. Vafiadis, and L. V. Van Horn, “Sodium, blood pressure, and cardiovascular disease: Further evidence supporting the American Heart Association sodium reduction recommendations,” *Circulation*, vol. 126, no. 24, pp. 2880–2889, 2012.
- [37] J. P. M. Biazus, J. C. C. Santana, R. R. Souza, E. Jordão, and E. B. Tambourgi, “Continuous extraction of α - and β -amylases from Zea mays malt in a PEG4000/CaCl₂ ATPS,” *J. Chromatogr. B Anal. Technol. Biomed. Life Sci.*, vol. 858, no. 1–2, pp. 227–233, 2007.
- [38] P. A. L. Wijethunga and H. Moon, “On-chip aqueous two-phase system (ATPS) formation, consequential self-mixing, and their influence on drop-to-drop aqueous two-phase extraction kinetics,” *J. Micromechanics Microengineering*, vol. 25, no. 9, p. 94002, 2015.
- [39] J. F. Liu, G. Bin Jiang, and J. Å. Jönsson, “Application of ionic liquids in analytical chemistry,” *TrAC - Trends Anal. Chem.*, vol. 24, no. 1, pp. 20–27, 2005.
- [40] N. Pal, S. Sharma, and S. Gupta, “Sensitive and rapid detection of pathogenic bacteria in small volumes using impedance spectroscopy technique,” *Biosens. Bioelectron.*, vol. 77, pp. 270–276, 2016.
- [41] Z. Zou, J. Kai, M. J. Rust, J. Han, and C. H. Ahn, “Functionalized nano interdigitated electrodes arrays on polymer with integrated microfluidics for direct

bio-affinity sensing using impedimetric measurement," *Sensors Actuators, A Phys.*, vol. 136, no. 2, pp. 518–526, 2007.

Biographical Information

Ali Farzbod received his bachelor of science degree in Aerospace engineering from the Amirkabir University of Technology in Tehran in 2012. He received his doctoral degree from University of Texas at Arlington in mechanical engineering in 2018. After finishing his bachelor studies, he got admitted directly to the Ph.D. program in Mechanical Engineering and joined Dr. Hyejin Moon's research laboratory, he started the research on 'reconfigurable electrochemical sensor using electrowetting on dielectric (EWOD) digital microfluidic functions.' during this time his research activities have been supported by NSF CAREER grant (ECCS-1254502).

His experience and knowledge in both design and fabrication of electrochemical biosensors and MEMS microfluidic devices made him versatile researcher in the field of healthcare diagnostics.

Ali future's goal is to build a blood testing company which will change the current business structure to a consumer-directed health care system eliminating the unnecessary costs and enabling trend analysis.